

High bandwidth (22 MHz) low offset (200 μ V) low-rail 5 V op amp



Features

- Gain bandwidth product 22 MHz, unity gain stable
- High accuracy input offset voltage: 50 μ V typ., 200 μ V max.
- Low input bias current: 2 pA typ.
- Low noise : 7 nV/ $\sqrt{\text{Hz}}$
- Slew rate : 11 V/ μ s
- Wide supply voltage range: 1.8 V to 5.5 V
- Output rail-to-rail, input low-rail
- Automotive grade and shutdown versions available
- Benefits:
 - High frequency signal conditioning
 - Optimized accuracy for low-side current sensing

Applications

- Low-side current measurement
- Photodiode amplifiers
- Automotive current measurement and sensor signal conditioning
- Strain gauges signal conditioning

Description

The **TSV7721**, **TSV7722** and **TSV7723** are single and dual 22 MHz-bandwidth unity-gain-stable amplifiers. The input offset voltage of 200 μ V max. (50 μ V typ.) at room temperature, optimized for common-mode close to ground makes the TSV772x ideal for low-side current measurements.

The TSV772x can operate from 1.8 V to 5.5 V single supply and it is fully specified on a load of 47 pF, therefore allowing easy usage as A/D converters input buffer.

The TSV772x series offers rail-to-rail output, excellent speed/power consumption ratio, and 22 MHz gain bandwidth product, while consuming just 1.7 mA at 5 V.

The devices also feature an ultra-low input bias current that enables connection to photodiodes and other sensors where current is the key value to be measured.

These features make the TSV772x series ideal for high-accuracy, high-bandwidth sensor interfaces.

| Maturity status link | Channel | Automotive | Package |
|----------------------|---------|------------|----------|
| TSV7721 | 1 | | SOT23-5 |
| | 1 | • | SOT23-5 |
| TSV7722 | 2 | | DFN8 |
| | 2 | | MiniSO8 |
| | 2 | | SO8 |
| | 2 | • | MiniSO8 |
| | 2 | • | SO8 |
| TSV7723 | 2 | | MiniSO10 |

| Related products | |
|------------------|---|
| TSV772 | Rail-to-rail 20 MHz amplifier |
| TSV792 | Rail-to-rail amplifier with higher GBW 50 MHz |
| TSB7192 | 22 MHz amplifier with 36 V supply voltage |

1 Pin description

1.1 TSV7721 single operational amplifier

Figure 1. Pin connections (top view)

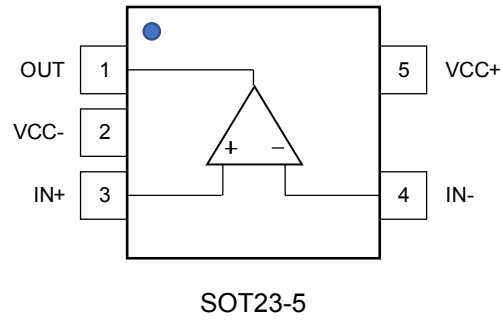
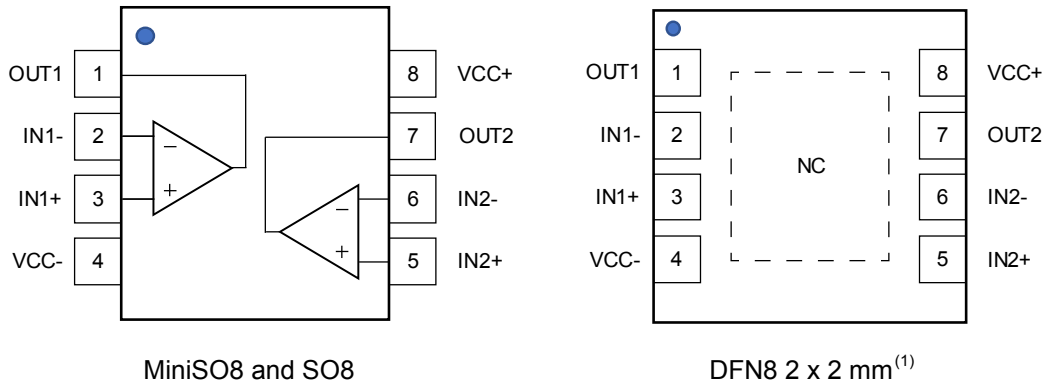


Table 1. Pin description

| Pin n° | Pin name | Description |
|--------|----------|-----------------------------|
| 1 | OUT | Output channel |
| 2 | VCC- | Negative supply voltage |
| 3 | IN+ | Non-inverting input channel |
| 4 | IN- | Inverting input channel |
| 5 | VCC+ | Positive supply voltage |

1.2 TSV7722 dual operational amplifier

Figure 2. Pin connections (top view)



1. The exposed pad of the DFN8 2x2 can be connected to VCC- or left floating.

Table 2. Pin description

| Pin n° | Pin name | Description |
|--------|----------|-------------------------------|
| 1 | OUT1 | Output channel 1 |
| 2 | IN1- | Inverting input channel 1 |
| 3 | IN1+ | Non-inverting input channel 1 |
| 4 | VCC- | Negative supply voltage |
| 5 | IN2+ | Non-inverting input channel 2 |
| 6 | IN2- | Inverting input channel 2 |
| 7 | OUT2 | Output channel 2 |
| 8 | VCC+ | Positive supply voltage |

1.3 TSV7723 dual operational amplifier with shutdown option

Figure 3. Pin connections (top view)

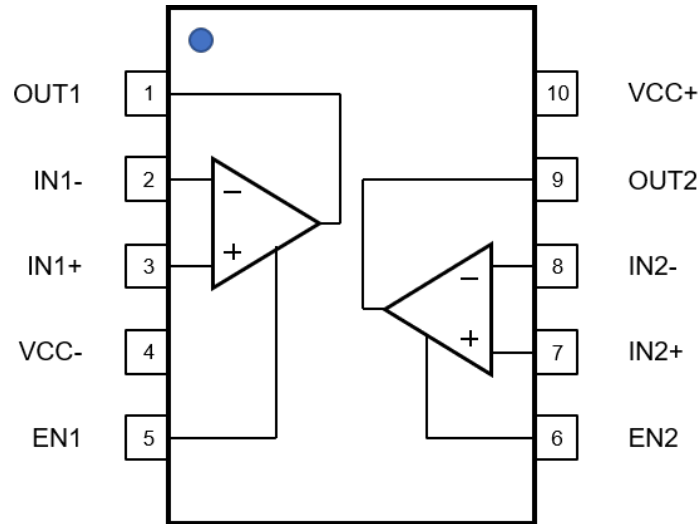


Table 3. Pin description

| Pin n° | Pin name | Description |
|--------|----------|--|
| 1 | OUT1 | Output channel 1 |
| 2 | IN1- | Inverting input channel 1 |
| 3 | IN1+ | Non-inverting input channel 1 |
| 4 | VCC- | Negative supply voltage |
| 5 | EN1 | Enable input channel 1 (amplifier in shutdown mode when EN pin connected to VCC-) |
| 6 | EN2 | Enable input channel 2 (amplifier in shutdown mode when EN pin connected to VCC-) |
| 7 | IN2+ | Non-inverting input channel 2 |
| 8 | IN2- | Inverting input channel 2 |
| 9 | OUT2 | Output channel 2 |
| 10 | VCC+ | Positive supply voltage |

2 Absolute maximum ratings and operating conditions

Table 4. Absolute maximum ratings

| Symbol | Parameter | Value | Unit |
|-------------|---|--|--------|
| V_{CC} | Supply voltage (referred to VCC- pin) ⁽¹⁾ | -0.3 to 6.0 | V |
| V_{id} | Differential input voltage ⁽²⁾ | $\pm V_{CC}$ | V |
| V_{IN} | Input pins input voltage ⁽³⁾ | $V_{CC-} - 0.3\text{ V}$ to $V_{CC+} + 0.3\text{ V}$ | V |
| I_{IN} | Input pins input current ⁽⁴⁾ | ± 10 | mA |
| T_{stg} | Storage temperature | -65 to 150 | °C |
| R_{th-ja} | Thermal resistance junction-to-ambient ⁽⁵⁾ | | °C / W |
| | SOT23-5 | 250 | |
| | DFN8 (2 mm x 2 mm) | 76 | |
| | MiniSO8 | 127 | |
| | MiniSO10 | 113 | |
| | SO8 | 113 | |
| T_j | Maximum junction temperature | 150 | °C |
| ESD | HBM: human body model ⁽⁶⁾ | 4 | kV |
| | CDM: charged device model ⁽⁷⁾ | 1.5 | kV |

1. All voltage values, except differential voltage, are with respect to VCC- pin.
2. The differential voltage is the non-inverting input terminal with respect to the inverting input terminal.
3. $V_{CC-} - V_{in}$ must not exceed 6 V, V_{in} must not exceed 6 V.
4. Input current must be limited by a resistor in series with the inputs.
5. R_{th} are typical values.
6. Human body model: the test HBM is done in accordance with the standards ESDA-JS-001-2017 and Q100-002
7. Charged device model: the test CDM is done in accordance with the standards ESDA-JS-002-2018 and Q100-011

Table 5. Operating conditions

| Symbol | Parameter | Min. | Max. | Value |
|------------|--------------------------------------|-----------------|-----------------|-------|
| V_{CC} | Supply voltage | 1.8 | 5.5 | V |
| V_{icm} | Common-mode input voltage range | $V_{CC-} - 0.1$ | $V_{CC+} - 1.1$ | V |
| T_{oper} | Operating free air temperature range | -40 | 125 | °C |

3 Electrical characteristics

Table 6. Electrical characteristics at $V_{CC+} = 5\text{ V}$, with $V_{CC-} = 0\text{ V}$, $V_{icm} = V_{CC} / 2$, $T = 25^\circ\text{C}$, and OUT pin connected to $V_{CC} / 2$ through $R_L = 10\text{ k}\Omega$ (unless otherwise specified)

| Symbol | Parameter | Conditions | Min. | Typ. | Max. | Unit |
|--------------------------|---|---|------|----------|-----------|------------------------------|
| DC Performance | | | | | | |
| V_{io} | Input offset voltage ($V_{icm} = 0\text{ V}$) | $T = 25^\circ\text{C}$ | | ± 50 | ± 250 | μV |
| | | $-40^\circ\text{C} < T < 125^\circ\text{C}$ | | | ± 650 | |
| $\Delta V_{io}/\Delta T$ | Input offset voltage drift ($V_{icm} = 0\text{ V}$) | $-40^\circ\text{C} < T < 125^\circ\text{C}$ | | | ± 4 | $\mu\text{V}/^\circ\text{C}$ |
| I_{ib} | Input bias current ($V_{OUT} = V_{CC}/2$) | $T = 25^\circ\text{C}$ | | 2 | | pA |
| | | $-40^\circ\text{C} < T < 125^\circ\text{C}$ | | 75 | | |
| I_{io} | Input offset current ($V_{OUT} = V_{CC}/2$) | $T = 25^\circ\text{C}$ | | 1 | | pA |
| | | $-40^\circ\text{C} < T < 125^\circ\text{C}$ | | 20 | | |
| CMR1 | Common-mode rejection ratio $20 \cdot \log(\Delta V_{icm}/\Delta V_{io})$, $V_{icm} = 0\text{ V}$ to $V_{CC-} - 1.1\text{ V}$, $R_L > 1\text{ M}\Omega$ | $T = 25^\circ\text{C}$ | 76 | 99 | | dB |
| | | $-40^\circ\text{C} < T < 125^\circ\text{C}$ | 74 | | | |
| CMR2 | Common-mode rejection ratio $20 \cdot \log(\Delta V_{icm}/\Delta V_{io})$, $V_{icm} = -0.1\text{ V}$ to $V_{CC-} - 1.1\text{ V}$, $R_L > 1\text{ M}\Omega$ | $T = 25^\circ\text{C}$ | 75 | | | dB |
| | | $-40^\circ\text{C} < T < 125^\circ\text{C}$ | 60 | | | |
| SVR | Supply voltage rejection ratio $20 \cdot \log(\Delta V_{CC}/\Delta V_{io})$, $V_{CC} = 1.8\text{ V}$ to 5.5 V , $V_{icm} = 0\text{ V}$, $R_L > 1\text{ M}\Omega$ | $T = 25^\circ\text{C}$ | 85 | 108 | | dB |
| | | $-40^\circ\text{C} < T < 125^\circ\text{C}$ | 80 | | | |
| A_{VD} | Large signal voltage gain $V_{OUT} = 0.3\text{ V}$ to ($V_{CC} - 0.3\text{ V}$) | $T = 25^\circ\text{C}$ | 111 | 130 | | dB |
| | | $-40^\circ\text{C} < T < 125^\circ\text{C}$ | 106 | | | |
| V_{OH} | High level output voltage ($V_{OH} = V_{CC} - V_{OUT}$) | $T = 25^\circ\text{C}$ | | | 15 | mV |
| | | $-40^\circ\text{C} < T < 125^\circ\text{C}$ | | | 25 | |
| V_{OL} | Low level output voltage | $T = 25^\circ\text{C}$ | | | 15 | mV |
| | | $-40^\circ\text{C} < T < 125^\circ\text{C}$ | | | 25 | |
| I_{OUT} | I_{sink} ($V_{OUT} = V_{CC}$) | $T = 25^\circ\text{C}$ | 50 | 70 | | mA |
| | | $-40^\circ\text{C} < T < 125^\circ\text{C}$ | 45 | | | |
| | I_{source} ($V_{OUT} = 0\text{ V}$) | $T = 25^\circ\text{C}$ | 45 | 65 | | |
| | | $-40^\circ\text{C} < T < 125^\circ\text{C}$ | 40 | | | |
| I_{CC} | Supply current (per channel, $V_{OUT} = V_{CC}/2$, $R_L > 1\text{ M}\Omega$) | $T = 25^\circ\text{C}$ | | 1.7 | 2.2 | mA |
| | | $-40^\circ\text{C} < T < 125^\circ\text{C}$ | | | 2.5 | |
| AC Performance | | | | | | |
| GBW | Gain bandwidth product | $C_L = 47\text{ pF}$ | 15 | 22 | | MHz |
| F_u | Unity gain frequency | | | 19.5 | | |
| Φ_m | Phase margin | | | 44 | | degrees |
| G_m | Gain margin | | | 8 | | dB |
| SR | Slew rate ⁽¹⁾ | | 8 | 11 | | $\text{V}/\mu\text{s}$ |

| Symbol | Parameter | Conditions | Min. | Typ. | Max. | Unit |
|--|---|--|------|------|------|------------------------|
| t_{rec} | Overload recovery time: t_{rec} is defined as delay between input voltage edge and V_{OUT} reaching 100 mV from initial value | | | 70 | | ns |
| t_s | Settling time | To 0.1%, $V_{in} = 1 V_{p-p}$ | | 270 | | ns |
| e_n | Equivalent input noise voltage | $f = 1 \text{ kHz}$ | | 13 | | nV/ $\sqrt{\text{Hz}}$ |
| | | $f = 10 \text{ kHz}$ | | 7 | | |
| C_S | Channel separation (for TSV7722 and TSV7723) | $f = 1 \text{ kHz}$ | | 120 | | dB |
| C_{in} | Input capacitance | Differential | | 6 | | pF |
| | | Common-mode | | 4.5 | | |
| Shutdown feature characteristics (TSV7723 only, op-amp in shutdown mode when EN input is low) | | | | | | |
| I_{CC} | Shutdown mode $V_{OUT} = V_{CC}/2$, $R_L > 1 \text{ M}\Omega$ | $T = 25^\circ\text{C}$ | | 2.5 | 60 | nA |
| | | $-40^\circ\text{C} < T < 85^\circ\text{C}$ | | | 450 | |
| | | $-40^\circ\text{C} < T < 125^\circ\text{C}$ | | | | 4 |
| t_{on} | Amplifier turn-on time (other channel already on) | $V_{OUT} = V_{CC-}$ to $V_{CC-} + 0.2 \text{ V}$ | | 2 | | μs |
| t_{init} | Initialization time (both channels off) | V_{OUT} to 200 mV of final value | | 7 | | μs |
| V_{IH} | EN logic high | | 2 | | | V |
| V_{IL} | EN logic low | | | | 0.8 | |
| I_{IH} | EN current high | $EN = V_{CC+}$ | | 1 | | pA |
| I_{IL} | EN current low | $EN = V_{CC-}$ | | 1 | | |
| I_{Oleak} | Output leakage in shutdown mode, $EN = V_{CC-}$ | $T = 25^\circ\text{C}$ | | 50 | | pA |
| | | $-40^\circ\text{C} < T < 125^\circ\text{C}$ | | 15 | | nA |

1. Slew rate value is calculated as the average between positive and negative slew rates.

Table 7. Electrical characteristics at $V_{CC+} = 3.3\text{ V}$, with $V_{CC-} = 0\text{ V}$, $V_{icm} = V_{CC} / 2$, $T = 25^\circ\text{C}$, and OUT pin connected to $V_{CC} / 2$ through $R_L = 10\text{ k}\Omega$ (unless otherwise specified)

| Symbol | Parameter | Conditions | Min. | Typ. | Max. | Unit | |
|--|--|---|--------------------------------------|----------|-----------|------------------------------|------------------------|
| DC Performance | | | | | | | |
| V_{io} | Input offset voltage ($V_{icm} = 0\text{ V}$) | $T = 25^\circ\text{C}$ | | ± 50 | ± 200 | μV | |
| | | $-40^\circ\text{C} < T < 125^\circ\text{C}$ | | | ± 600 | | |
| $\Delta V_{io}/\Delta T$ | Input offset voltage drift ($V_{icm} = 0\text{ V}$) | $-40^\circ\text{C} < T < 125^\circ\text{C}$ | | | ± 4 | $\mu\text{V}/^\circ\text{C}$ | |
| I_{ib} | Input bias current ($V_{OUT} = V_{CC}/2$) | $T = 25^\circ\text{C}$ | | 1.8 | | pA | |
| | | $-40^\circ\text{C} < T < 125^\circ\text{C}$ | | 60 | | | |
| I_{io} | Input offset current ($V_{OUT} = V_{CC}/2$) | $T = 25^\circ\text{C}$ | | 1 | | pA | |
| | | $-40^\circ\text{C} < T < 125^\circ\text{C}$ | | 20 | | | |
| CMR1 | Common-mode rejection ratio $20 \cdot \log(\Delta V_{icm}/\Delta V_{io})$, $V_{icm} = 0\text{ V}$ to $V_{CC-} - 1.1\text{ V}$, $R_L > 1\text{ M}\Omega$ | $T = 25^\circ\text{C}$ | 75 | 96 | | dB | |
| | | $-40^\circ\text{C} < T < 125^\circ\text{C}$ | 71 | | | | |
| CMR2 | Common-mode rejection ratio $20 \cdot \log(\Delta V_{icm}/\Delta V_{io})$, $V_{icm} = -0.1\text{ V}$ to $V_{CC-} - 1.1\text{ V}$, $R_L > 1\text{ M}\Omega$ | $T = 25^\circ\text{C}$ | 73 | | | dB | |
| | | $-40^\circ\text{C} < T < 125^\circ\text{C}$ | 57 | | | | |
| A_{VD} | Large signal voltage gain $V_{OUT} = 0.3\text{ V}$ to ($V_{CC-} - 0.3\text{ V}$) | $T = 25^\circ\text{C}$ | 107 | 128 | | dB | |
| | | $-40^\circ\text{C} < T < 125^\circ\text{C}$ | 103 | | | | |
| V_{OH} | High level output voltage ($V_{OH} = V_{CC} - V_{OUT}$) | $T = 25^\circ\text{C}$ | | | 15 | mV | |
| | | $-40^\circ\text{C} < T < 125^\circ\text{C}$ | | | 25 | | |
| V_{OL} | Low level output voltage | $T = 25^\circ\text{C}$ | | | 15 | mV | |
| | | $-40^\circ\text{C} < T < 125^\circ\text{C}$ | | | 25 | | |
| I_{OUT} | I_{sink} ($V_{OUT} = V_{CC}$) | $T = 25^\circ\text{C}$ | 50 | 70 | | mA | |
| | | $-40^\circ\text{C} < T < 125^\circ\text{C}$ | 45 | | | | |
| | I_{source} ($V_{OUT} = 0\text{ V}$) | $T = 25^\circ\text{C}$ | 45 | 65 | | | |
| | | $-40^\circ\text{C} < T < 125^\circ\text{C}$ | 40 | | | | |
| I_{CC} | Supply current (per channel, $V_{OUT} = V_{CC}/2$, $R_L > 1\text{ M}\Omega$) | $T = 25^\circ\text{C}$ | | 1.7 | 2.2 | mA | |
| | | $-40^\circ\text{C} < T < 125^\circ\text{C}$ | | | 2.5 | | |
| AC Performance | | | | | | | |
| GBW | Gain bandwidth product | | 14 | 21 | | MHz | |
| F_u | Unity gain frequency | | | 18.5 | | | |
| Φ_m | Phase margin | $C_L = 47\text{ pF}$ | | 42 | | degrees | |
| G_m | Gain margin | | | 8 | | dB | |
| SR | Slew rate ⁽¹⁾ | | | 7.7 | 11 | | $\text{V}/\mu\text{s}$ |
| t_s | Settling time | | To 0.1%, $V_{in} = 1\text{ V}_{p-p}$ | | 210 | | ns |
| e_n | Equivalent input noise voltage | $f = 1\text{ kHz}$ | | 13 | | $\text{nV}/\sqrt{\text{Hz}}$ | |
| | | $f = 10\text{ kHz}$ | | 7 | | | |
| C_S | Channel separation (for TSV7722 and TSV7723) | $f = 1\text{ kHz}$ | | 120 | | dB | |
| Shutdown feature characteristics (TSV7723 only, op-amp in shutdown mode when EN input is low) | | | | | | | |
| I_{CC} | Shutdown mode $V_{OUT} = V_{CC}/2$, $R_L > 1\text{ M}\Omega$ | $T = 25^\circ\text{C}$ | | 2.5 | 60 | nA | |
| | | $-40^\circ\text{C} < T < 85^\circ\text{C}$ | | | 450 | | |

| Symbol | Parameter | Conditions | Min. | Typ. | Max. | Unit |
|-------------|---|---|------|------|------|---------------|
| I_{CC} | Shutdown mode $V_{OUT} = V_{CC}/2$, $R_L > 1\text{ M}\Omega$ | $-40^\circ\text{C} < T < 125^\circ\text{C}$ | | | 4 | μA |
| t_{on} | Amplifier turn-on time (other channel already on) | $V_{OUT} = V_{CC-}$ to $V_{CC-} + 0.2\text{ V}$ | | 2 | | μs |
| t_{init} | Initialization time (both channels off) | V_{OUT} to 200 mV of final value | | 11 | | μs |
| V_{IH} | EN logic high | | 2 | | | V |
| V_{IL} | EN logic low | | | | 0.8 | |
| I_{IH} | EN current high | $EN = V_{CC+}$ | | 1 | | pA |
| I_{IL} | EN current low | $EN = V_{CC-}$ | | 1 | | |
| I_{Oleak} | Output leakage in shutdown mode, $EN = V_{CC-}$ | $T = 25^\circ\text{C}$ | | 50 | | pA |
| | | $-40^\circ\text{C} < T < 125^\circ\text{C}$ | | 15 | | nA |

1. Slew rate value is calculated as the average between positive and negative slew rates.

Table 8. Electrical characteristics at $V_{CC+} = 1.8\text{ V}$, with $V_{CC-} = 0\text{ V}$, $V_{icm} = 0.7\text{ V}$, $T = 25^\circ\text{C}$, and OUT pin connected to V_{CC-} / 2 through $R_L = 10\text{ k}\Omega$ (unless otherwise specified)

| Symbol | Parameter | Conditions | Min. | Typ. | Max. | Unit |
|--|--|---|------|----------|-----------|------------------------------|
| DC Performance | | | | | | |
| V_{io} | Input offset voltage ($V_{icm} = 0\text{ V}$) | $T = 25^\circ\text{C}$ | | ± 50 | ± 250 | μV |
| | | $-40^\circ\text{C} < T < 125^\circ\text{C}$ | | | ± 650 | |
| $\Delta V_{io}/\Delta T$ | Input offset voltage drift ($V_{icm} = 0\text{ V}$) | $-40^\circ\text{C} < T < 125^\circ\text{C}$ | | | ± 4 | $\mu\text{V}/^\circ\text{C}$ |
| I_{ib} | Input bias current ($V_{OUT} = V_{CC}/2$) | $T = 25^\circ\text{C}$ | | 1 | | pA |
| | | $-40^\circ\text{C} < T < 125^\circ\text{C}$ | | 40 | | |
| I_{io} | Input offset current ($V_{OUT} = V_{CC}/2$) | $T = 25^\circ\text{C}$ | | 1 | | pA |
| | | $-40^\circ\text{C} < T < 125^\circ\text{C}$ | | 15 | | |
| CMR1 | Common-mode rejection ratio $20 \cdot \log(\Delta V_{icm}/\Delta V_{io})$, $V_{icm} = 0\text{ V}$ to $V_{CC-} - 1.1\text{ V}$, $R_L > 1\text{ M}\Omega$ | $T = 25^\circ\text{C}$ | 72 | 93 | | dB |
| | | $-40^\circ\text{C} < T < 125^\circ\text{C}$ | 68 | | | |
| CMR2 | Common-mode rejection ratio $20 \cdot \log(\Delta V_{icm}/\Delta V_{io})$, $V_{icm} = -0.1\text{ V}$ to $V_{CC-} - 1.1\text{ V}$, $R_L > 1\text{ M}\Omega$ | $T = 25^\circ\text{C}$ | 70 | | | dB |
| | | $-40^\circ\text{C} < T < 125^\circ\text{C}$ | 52 | | | |
| A_{VD} | Large signal voltage gain $V_{OUT} = 0.3\text{ V}$ to ($V_{CC-} - 0.3\text{ V}$) | $T = 25^\circ\text{C}$ | 101 | 122 | | dB |
| | | $-40^\circ\text{C} < T < 125^\circ\text{C}$ | 97 | | | |
| V_{OH} | High level output voltage ($V_{OH} = V_{CC} - V_{OUT}$) | $T = 25^\circ\text{C}$ | | | 15 | mV |
| | | $-40^\circ\text{C} < T < 125^\circ\text{C}$ | | | 25 | |
| V_{OL} | Low level output voltage | $T = 25^\circ\text{C}$ | | | 15 | mV |
| | | $-40^\circ\text{C} < T < 125^\circ\text{C}$ | | | 25 | |
| I_{OUT} | I_{sink} ($V_{OUT} = V_{CC}$) | $T = 25^\circ\text{C}$ | 35 | 42 | | mA |
| | | $-40^\circ\text{C} < T < 125^\circ\text{C}$ | 20 | | | |
| | I_{source} ($V_{OUT} = 0\text{ V}$) | $T = 25^\circ\text{C}$ | 20 | 32 | | |
| | | $-40^\circ\text{C} < T < 125^\circ\text{C}$ | 10 | | | |
| I_{CC} | Supply current (per channel, $V_{OUT} = V_{CC} / 2$, $R_L > 1\text{ M}\Omega$) | $T = 25^\circ\text{C}$ | | 1.7 | 2.2 | mA |
| | | $-40^\circ\text{C} < T < 125^\circ\text{C}$ | | | 2.5 | |
| AC Performance | | | | | | |
| GBW | Gain bandwidth product | $C_L = 47\text{ pF}$ | | 14 | 21 | MHz |
| F_u | Unity gain frequency | | | | 18 | |
| Φ_m | Phase margin | | | | 41 | degrees |
| G_m | Gain margin | | | | 8 | dB |
| SR | Slew rate ⁽¹⁾ | | | | 7.6 | 11 |
| e_n | Equivalent input noise voltage | $f = 1\text{ kHz}$ | | 13 | | $\text{nV}/\sqrt{\text{Hz}}$ |
| | | $f = 10\text{ kHz}$ | | 7 | | |
| C_S | Channel separation (for TSV7722 and TSV7723) | $f = 1\text{ kHz}$ | | 120 | | dB |
| Shutdown feature characteristics (TSV7723 only, op-amp in shutdown mode when EN input is low) | | | | | | |
| I_{CC} | Shutdown mode $V_{OUT} = V_{CC}/2$, $R_L > 1\text{ M}\Omega$ | $T = 25^\circ\text{C}$ | | 2.5 | 60 | nA |
| | | $-40^\circ\text{C} < T < 85^\circ\text{C}$ | | | 450 | |

| Symbol | Parameter | Conditions | Min. | Typ. | Max. | Unit |
|-------------|---|---|------|------|------|---------------|
| I_{CC} | Shutdown mode $V_{OUT} = V_{CC}/2$, $R_L > 1\text{ M}\Omega$ | $-40^\circ\text{C} < T < 125^\circ\text{C}$ | | | 4 | μA |
| t_{on} | Amplifier turn-on time (other channel already on) | $V_{OUT} = V_{CC} - \text{to } V_{CC} - + 0.2\text{ V}$ | | 1.5 | | μs |
| t_{init} | Initialization time (both channels off) | V_{OUT} to 200 mV of final value | | 38 | | μs |
| V_{IH} | EN logic high | | 1.2 | | | V |
| V_{IL} | EN logic low | | | | 0.6 | |
| I_{IH} | EN current high | $EN = V_{CC+}$ | | 1 | | pA |
| I_{IL} | EN current low | $EN = V_{CC-}$ | | 1 | | |
| I_{Oleak} | Output leakage in shutdown mode, $EN = V_{CC-}$ | $T = 25^\circ\text{C}$ | | 50 | | pA |
| | | $-40^\circ\text{C} < T < 125^\circ\text{C}$ | | 15 | | nA |

1. Slew rate value is calculated as the average between positive and negative slew rates.

4 Typical performance characteristics

$R_L = 10\text{ k}\Omega$ connected to $V_{CC} / 2$ and $C_L = 47\text{ pF}$, unless otherwise specified.

Figure 4. Supply current vs. supply voltage

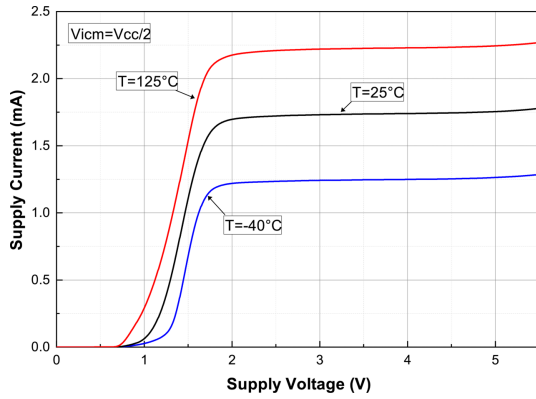


Figure 5. Input offset voltage distribution at $V_{CC} = 5\text{ V}$

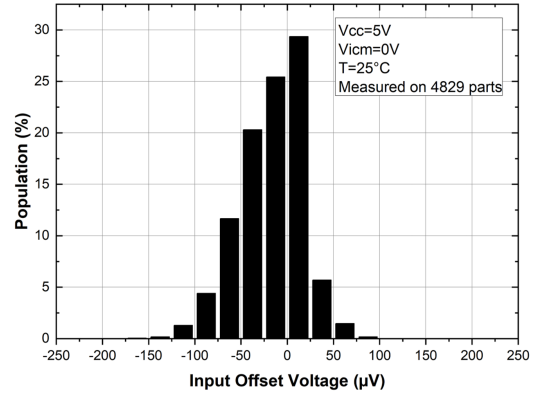


Figure 6. Input offset voltage distribution at $V_{CC} = 1.8\text{ V}$

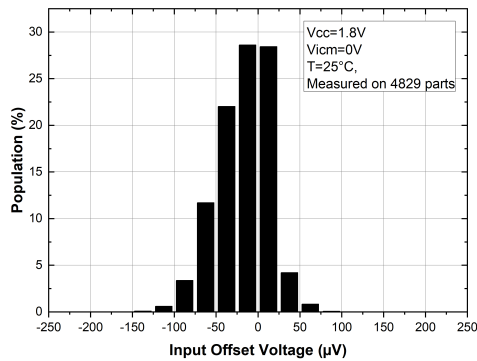


Figure 7. Input offset voltage vs. temperature at $V_{CC} = 5\text{ V}$

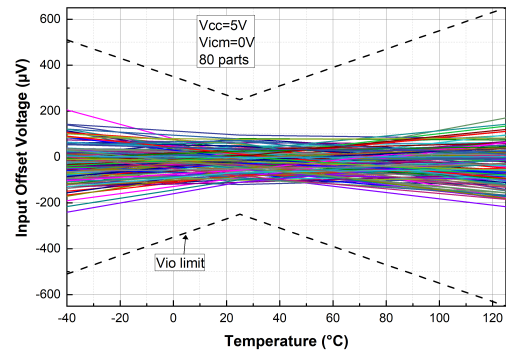


Figure 8. Input offset voltage vs. temperature at $V_{CC}=1.8\text{ V}$

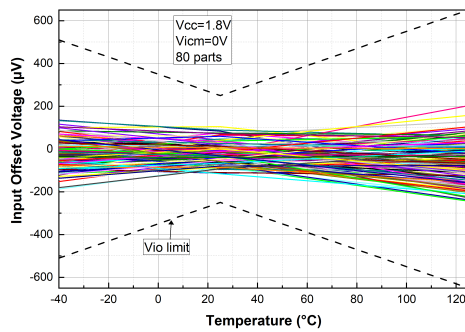


Figure 9. Input offset voltage thermal coeff. at $V_{CC}=5\text{ V}$

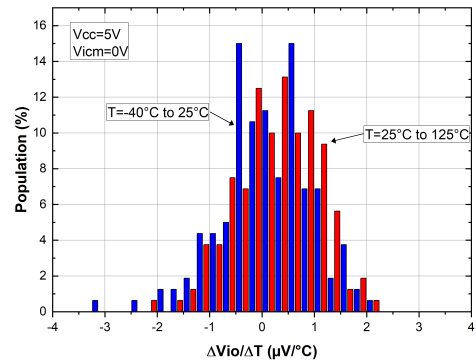


Figure 10. Input offset voltage thermal coefficient at $V_{CC}=1.8\text{ V}$

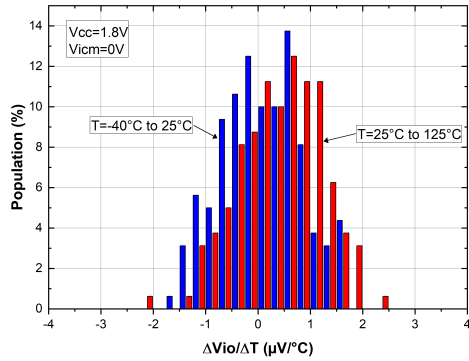


Figure 11. Input offset voltage vs. supply voltage

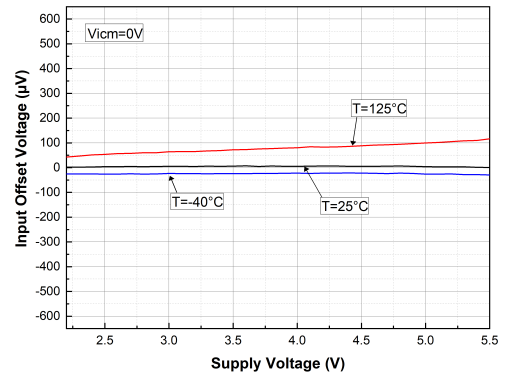


Figure 12. Input offset voltage vs. common-mode voltage at $V_{CC} = 5\text{ V}$

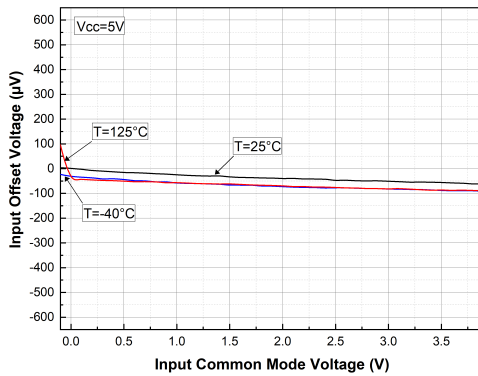


Figure 13. Input offset voltage vs. common-mode voltage at $V_{CC} = 1.8\text{ V}$

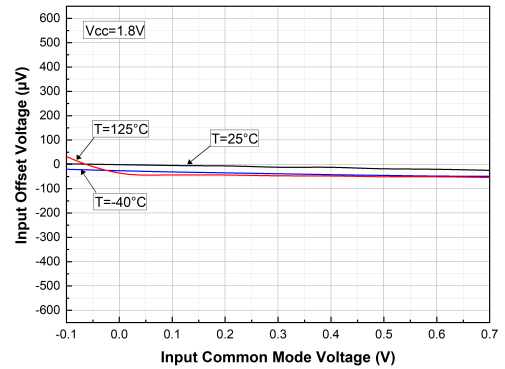


Figure 14. Input bias current vs. temp. at $V_{ICM} = V_{CC} / 2$

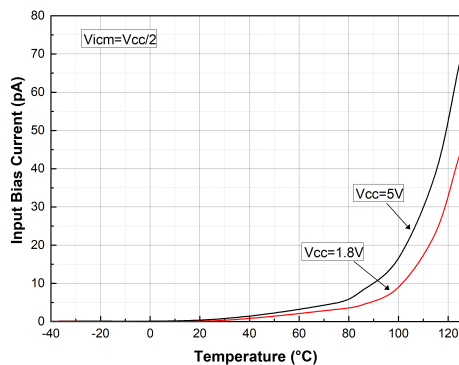


Figure 15. Input bias current vs. common-mode voltage at $V_{CC} = 5\text{ V}$

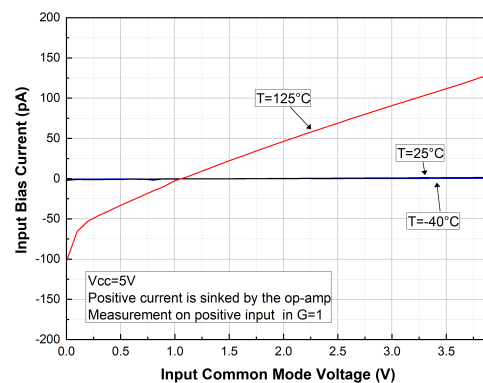


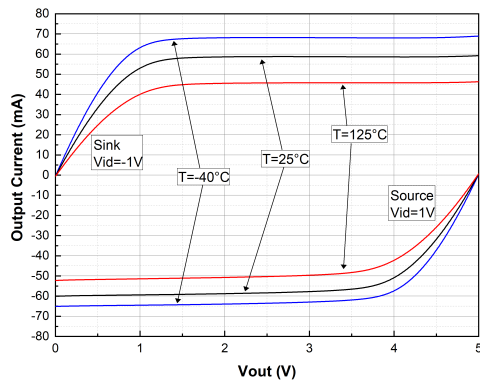
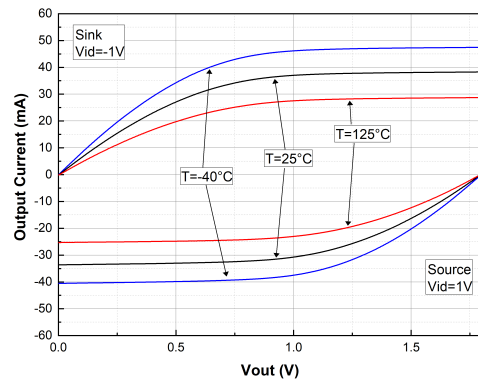
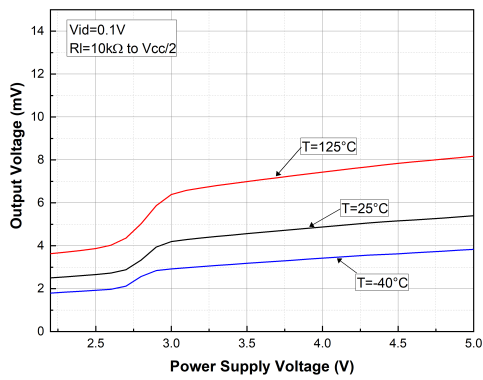
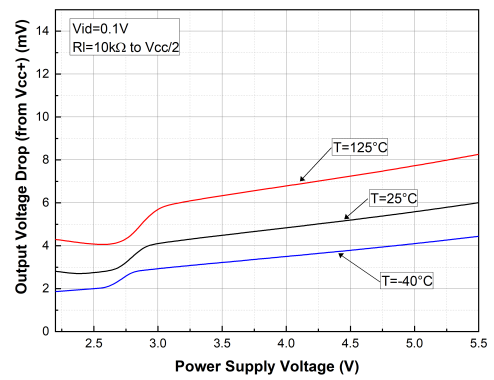
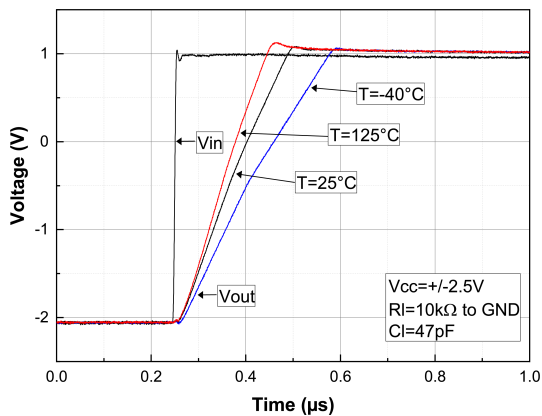
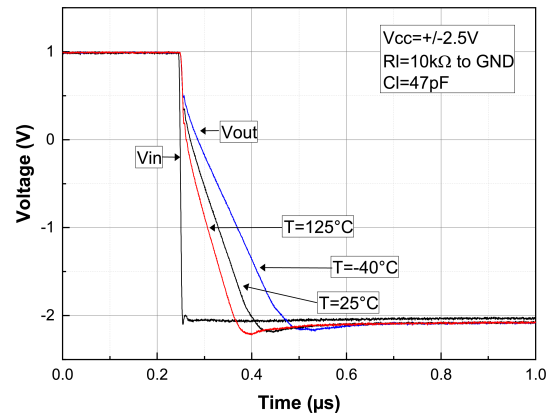
Figure 16. Output current vs. output voltage at $V_{CC} = 5\text{ V}$

Figure 17. Output current versus output voltage at $V_{CC} = 1.8\text{ V}$

Figure 18. Output saturation voltage (V_{OL}) vs. supply voltage

Figure 19. Output saturation voltage (V_{OH}) vs. supply voltage

Figure 20. Positive slew rate at $V_{CC} = 5\text{ V}$

Figure 21. Negative slew rate at $V_{CC} = 5\text{ V}$


Figure 22. Slew rate vs. V_{CC}

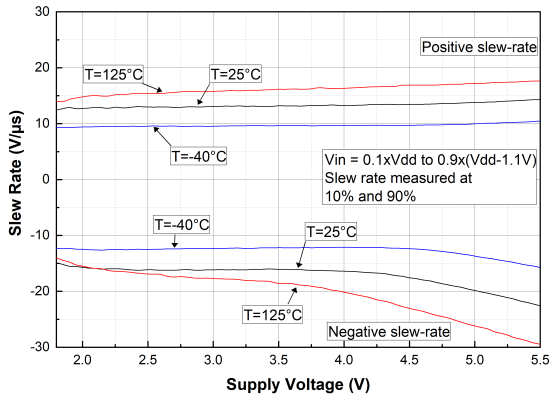


Figure 23. Open loop bode diagram at $V_{CC} = 5\text{ V}$

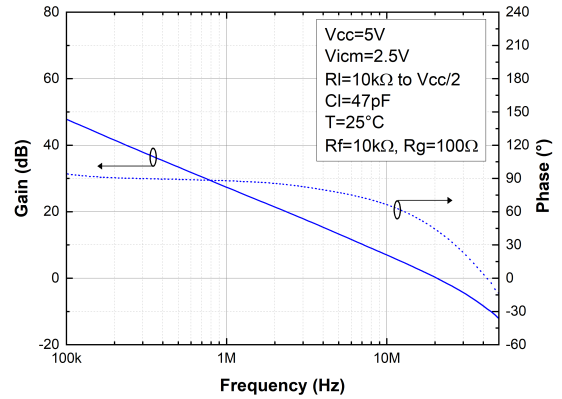


Figure 24. Open loop bode diagram at $V_{CC} = 1.8\text{ V}$

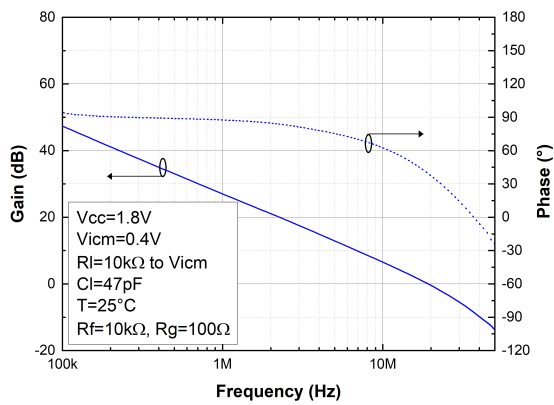


Figure 25. Closed loop bode diagram at $V_{CC} = 5\text{ V}$

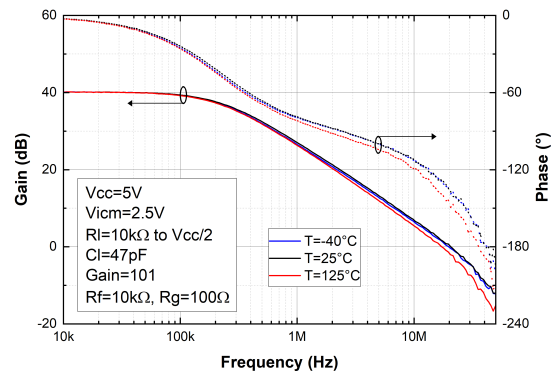


Figure 26. Closed loop bode diagram at $V_{CC} = 1.8\text{ V}$

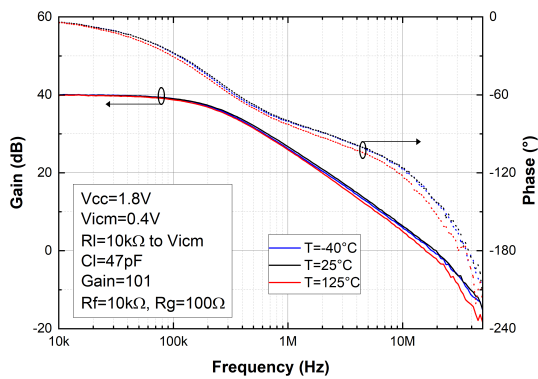


Figure 27. Phase margin vs. common-mode voltage and load current at $V_{CC} = 5\text{ V}$

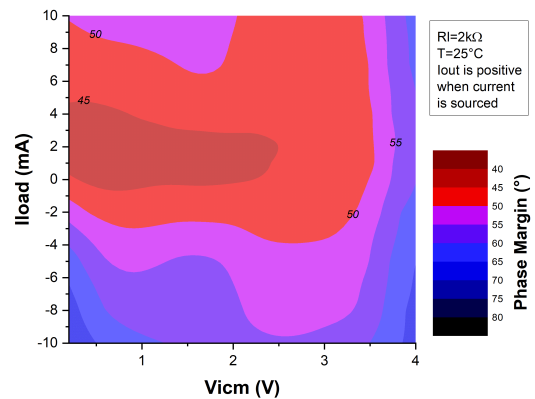


Figure 28. Phase margin vs. capacitive load

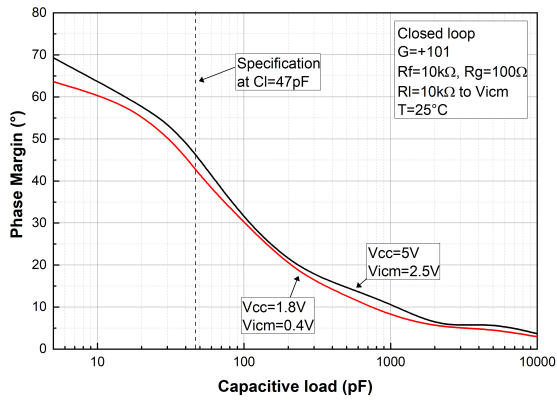


Figure 29. Small step response at $V_{CC} = 5\text{V}$

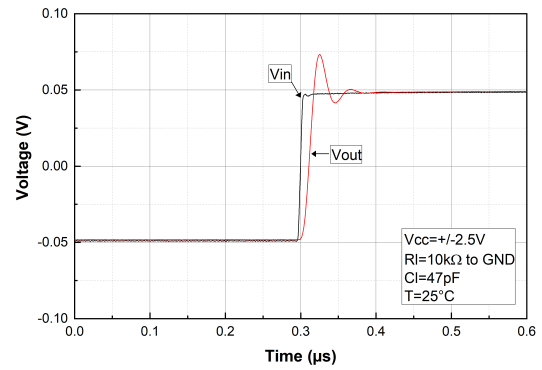


Figure 30. Small step response at $V_{CC} = 1.8\text{V}$

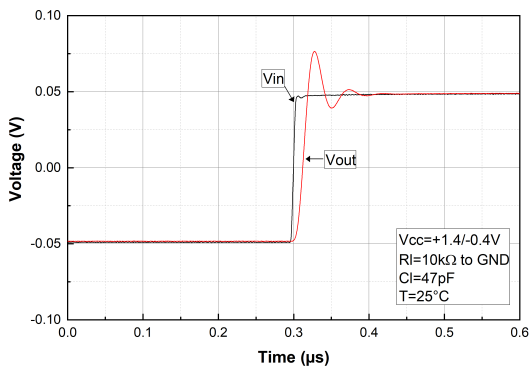


Figure 31. Desaturation from low rail at $V_{CC} = 5\text{V}$

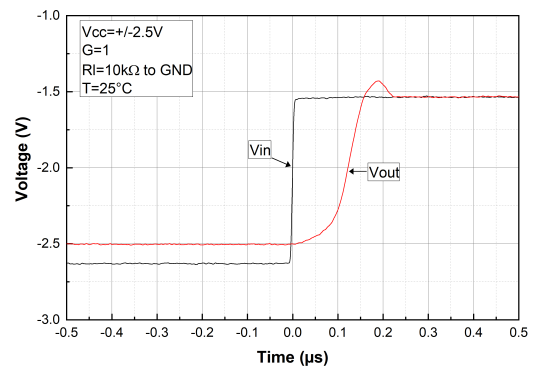


Figure 32. Desaturation from high rail at $V_{CC} = 5\text{V}$

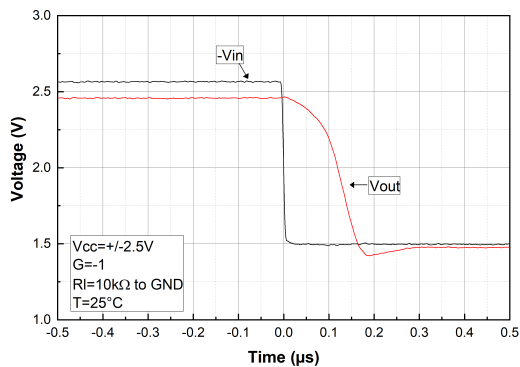


Figure 33. Settling time output high to low at $V_{CC} = 5\text{V}$

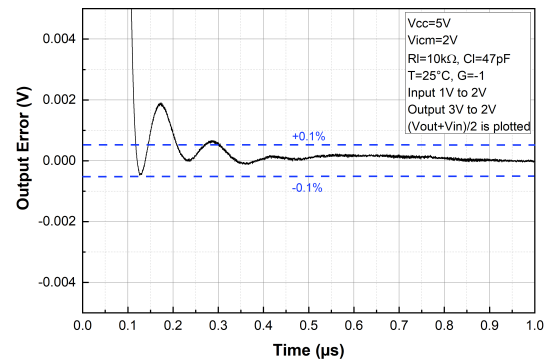


Figure 34. Settling time output low to high at $V_{CC} = 5\text{ V}$

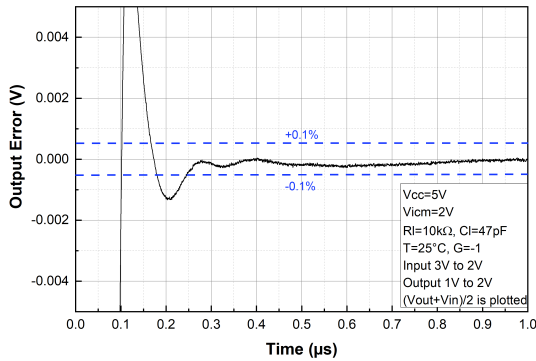


Figure 35. Small step overshoot vs. load capacitance

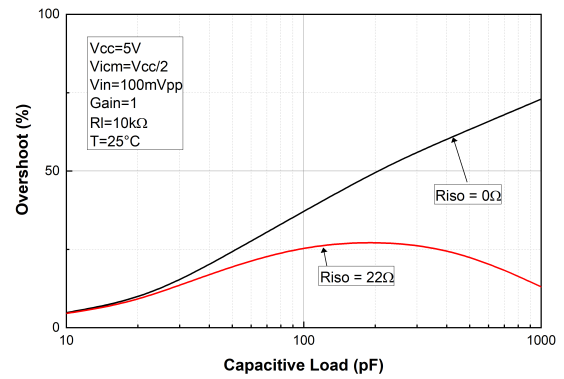


Figure 36. Linearity vs. load resistance at $V_{CC} = 5\text{ V}$

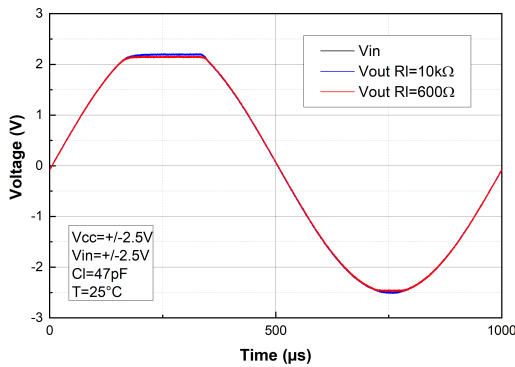


Figure 37. Noise vs. frequency

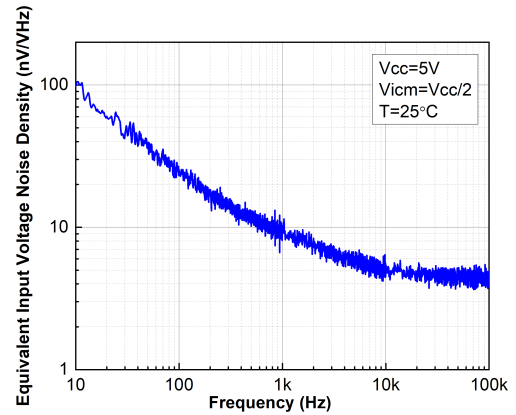


Figure 38. Noise versus time at $V_{CC} = 5\text{ V}$

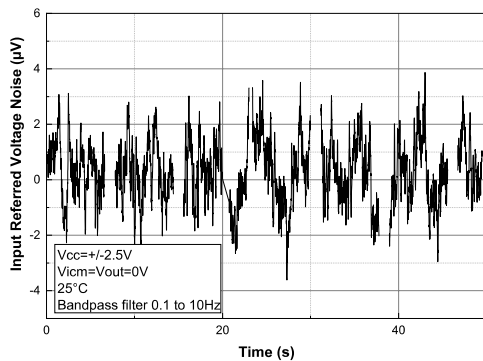


Figure 39. THD+N vs. frequency

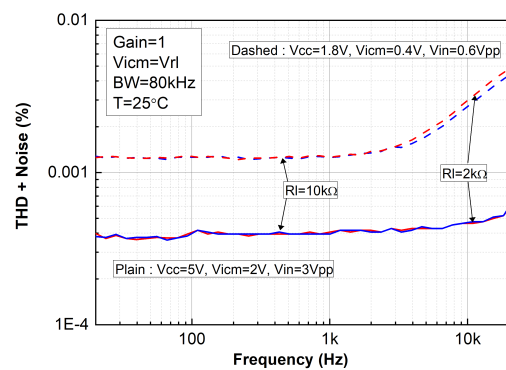


Figure 40. THD+N vs. output voltage

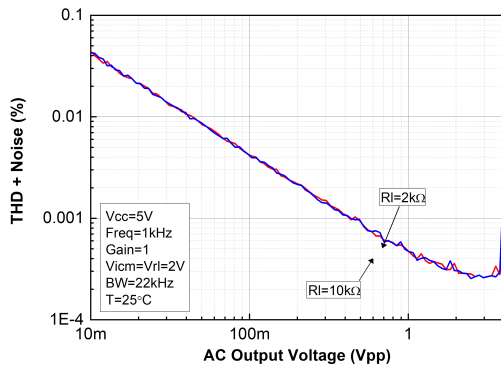


Figure 41. CMRR vs. frequency at $V_{CC} = 5V$

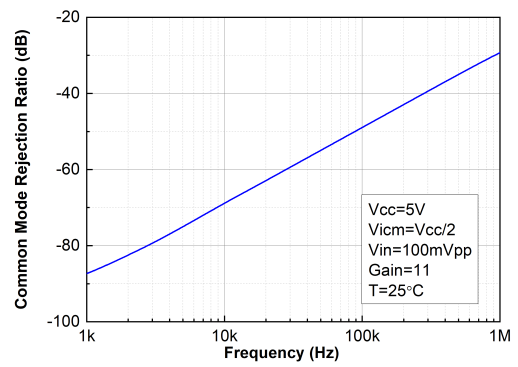


Figure 42. PSRR vs. frequency at $V_{CC} = 5V$

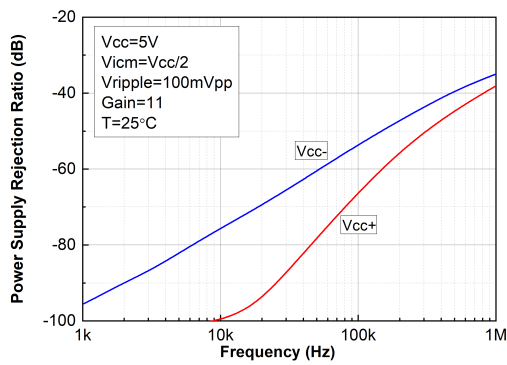


Figure 43. Supply current vs. supply voltage in shutdown mode

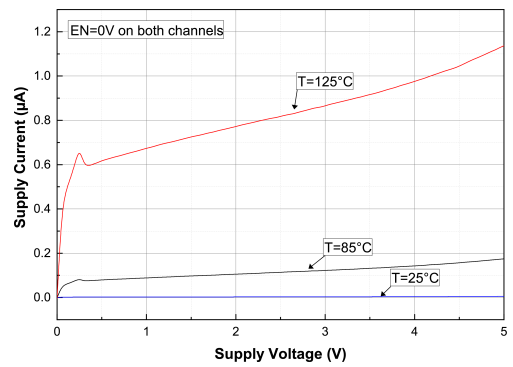


Figure 44. Turn-on time at $V_{CC} = 5V$

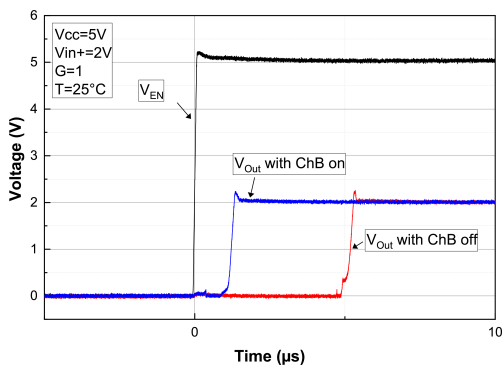
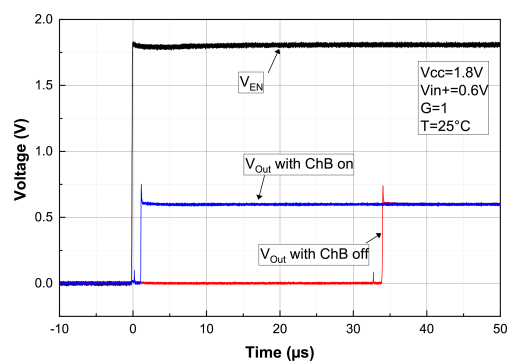


Figure 45. Turn-on time at $V_{CC} = 1.8V$



5 Application information

5.1 Operating voltages

The TSV7722 device can operate from 1.8 to 5.5 V. The parameters are fully specified at 1.8 V, 3.3 V and 5 V power supplies. However, the parameters are very stable over the full V_{CC} range and several characterization curves show the TSV7722 device characteristics over the full operating range. Additionally, the main specifications are guaranteed in extended temperature range from - 40 to 125 °C.

The TSV7722 device is low rail input, and rail-to-rail output. The common-mode operating range is from $V_{CC-} - 0.1$ V, to $V_{CC+} - 1.1$ V. The op amp V_{io} is trimmed at $V_{CC} = 3.3$ V, $V_{icm} = 0$ V, and thus the DC precision is optimized for operation with V_{icm} close to V_{CC-} .

5.2 Input offset voltage drift over the temperature

The maximum input voltage drift overtemperature is defined as the offset variation related to the offset value measured at 25 °C. The operational amplifier is one of the main circuits of the signal conditioning chain, and the amplifier input offset is a major contributor to the chain accuracy. The signal chain accuracy at 25 °C can be compensated during production at application level. The maximum input voltage drift overtemperature enables the system designer to anticipate the effect of temperature variations.

The maximum input voltage drift overtemperature is computed using the following equation:

$$\frac{\Delta V_{io}}{\Delta T} = \max \left| \frac{V_{io}(T) - V_{io}(25^{\circ}C)}{T - 25^{\circ}C} \right|$$

Where $T = - 40$ °C and 125 °C.

The TSV7721, TSV7722, TSV7723 datasheet maximum value is guaranteed by measurements on a representative sample size ensuring a C_{pk} (process capability index) greater than 1.3.

5.3 Unused channel

When one of the two channels of the TSV7722 is not used, it must be properly connected in order to avoid internal oscillations that can negatively impact the signal integrity on the other channel, as well as the current consumption. Two different configurations can be used:

Gain configuration: the channel can be set in gain, the input can be set to any voltage within the V_{icm} operating range.

Comparator configuration: the channel can be set to a comparator configuration (without negative feedback). In this case, positive and negative inputs can be set to any value provided these values are significantly different (100 mV or more, to avoid oscillation between positive and negative state).

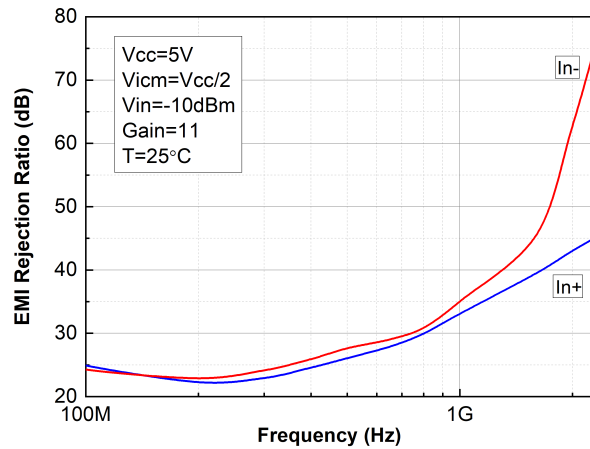
5.4 EMI rejection

The electromagnetic interference (EMI) rejection ratio, or EMIRR, describes the EMI immunity of operational amplifiers. An adverse effect that is common to many op amps is a change in the offset voltage as a result of RF signal rectification. EMIRR is defined in Eq. (2):

$$EMIRR = 20 \cdot \log \left(\frac{V_{in\ pp}}{\Delta V_{io}} \right)$$

The TSV7722 has been specially designed to minimize susceptibility to EMIRR and shows a low sensitivity. As can be seen in Figure 46. EMIRR on $In+$, $In-$ and Out pins, EMI rejection ratio has been measured on both inputs and output, from 400 MHz to 2.4 GHz.

Figure 46. EMIRR on In+, In- and Out pins



EMIRR performances might be improved by adding small capacitances (in the pF range) on the inputs, power supply and output pins.

These capacitances help to minimize the impedance of these nodes at high frequencies.

5.5 Maximum power dissipation

The usable output load current drive is limited by the maximum power dissipation allowed by the device package. The absolute maximum junction temperature for the TSV7722 is 150 °C. The junction temperature can be estimated as follows:

$$T_J = P_D \times \theta_{JA} + T_A$$

T_J is the die junction temperature

P_D is the power dissipated in the package

θ_{JA} is the junction to ambient thermal resistance of the package.

T_A is the ambient temperature.

The power dissipated in the package P_D is the sum of the quiescent power dissipated and the power dissipated by the output stage transistor. It is calculated as follows:

$$P_D = (V_{CC} \times I_{CC}) + (V_{CC+} - V_{OUT}) \times I_{Load} \text{ when the op amp is sourcing the current.}$$

$$P_D = (V_{CC} \times I_{CC}) + (V_{OUT} - V_{CC-}) \times I_{Load} \text{ when the op amp is sinking the current.}$$

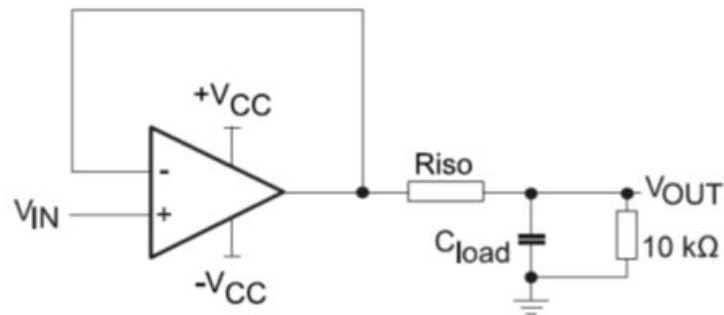
Do not exceed the 150 °C maximum junction temperature for the device. Exceeding the junction temperature limit can cause degradation in the parametric performance or even destroy the device.

5.6 Capacitive load and stability

Stability analysis must be performed for large capacitive loads over 47 pF; increasing the load capacitance to high values produces gain peaking in the frequency response, with overshoot and ringing in the step response.

Generally, unity gain configuration is the worst situation for stability and the ability to drive large capacitive loads. For additional capacitive load drive capability in unity-gain configuration, stability can be improved by inserting a small resistor R_{ISO} (10 Ω to 22 Ω) in series with the output (see [Figure 35. Small step overshoot vs. load capacitance](#)). This resistor significantly reduces ringing while maintaining DC performance for purely capacitive loads. However, if there is a resistive load in parallel with the capacitive load, a voltage divider is created introducing a gain error at the output and slightly reducing the output swing. The error introduced is proportional to the ratio R_{ISO} / R_L . R_{ISO} modifies the maximum capacitive load acceptable from a stability point of view, as described in [Figure 47. Test configuration for \$R_{ISO}\$](#) :

Figure 47. Test configuration for R_{ISO}

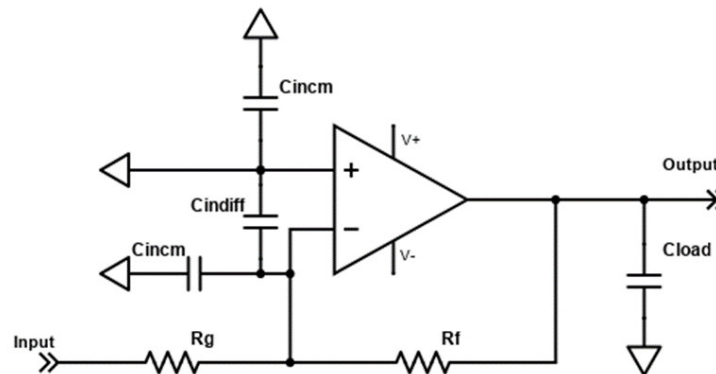


Please note that $R_{ISO} = 22 \Omega$ is sufficient to make the TSV7722 stable whatever the capacitive load.

5.7 Resistor values for high speed op amp design

Due to its high gain bandwidth product (GBP), this op amp is particularly sensitive to parasitic impedances. Board parasitics should be taken into account in any sensitive design. Indeed, excessive parasitic (both capacitive and inductive) in the op amp frequency range can alter performances and stability. These issues can often be mitigated by lowering the resistive impedances. More specifically, the RC network created by the schematic resistors (R_f and R_g) and the parasitic capacitances of both the op amp (as documented in Table 6 to Table 8 and illustrated in Figure 48) and the PCB can generate a pole below or in the same order of magnitude than the closed-loop bandwidth of the circuit. In this case, the feedback circuit is not able to fully play its role at high frequency, and the application can be unstable. This issue can happen when the schematic gain is low (typically < 5), or the device is used in follower mode with a resistor in the feedback. In these cases, it is advised to use a low value feedback resistor (R_f), typically $1 \text{ k}\Omega$.

Figure 48. Inverting amplifier configuration with parasitic input capacitances

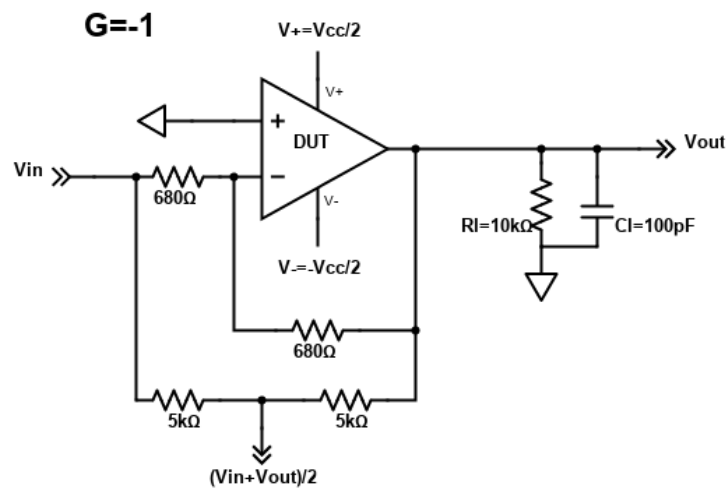


Also, some designs use an input resistor on the positive input, generally of the same value than the input resistance on the negative input. This resistor can be useful to balance the input currents on the positive and negative inputs, and reduce the impact of those input currents on precision. However, this is not useful on the TSV7722 as the input currents are very low. Furthermore, this resistor can also interact with the input capacitances to generate a pole. The frequency of this pole should be kept higher than the closed-loop bandwidth frequency. The macromodel provided takes into account the circuit parasitic capacitors. Thus, a transient SPICE simulation (100 mV step) is an easy way to evaluate the stability of the application. However, this cannot replace a hardware evaluation of the application circuit.

5.8 Settling time

Settling time in an application can be defined as the amount of time between the input changes, and the output reaching its final value. It is usually defined with a given tolerance, so the output stability is reached when the output stays within the given range around the final value. In Figure 33. Settling time output high to low at $V_{CC} = 5\text{ V}$ and Figure 34. Settling time output low to high at $V_{CC} = 5\text{ V}$, the settling time is measured in an inverting configuration, using the so-called “false summing node” circuit.

Figure 49. Settling time measurement configuration



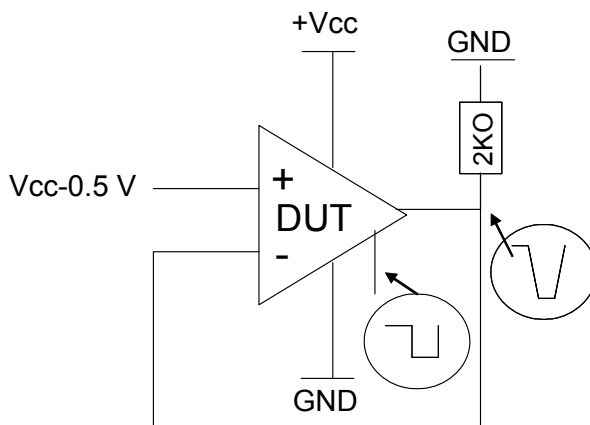
This circuit is used with a step input voltage from a positive or negative value, to 0 V. The measurement point being $(V_{in} + V_{out}) / 2$, and V_{out} being in an ideal circuit equal to V_{in} ; the measurement point gives half of the error on V_{out} , comparatively to V_{in} . This error is compared to the tolerance, 0.1% for this circuit, to deduce the settling time. This characteristic is particularly useful when driving an ADC. It is related to the slew rate, GBP and stability of the circuit. It also varies with the circuit gain, the circuit load, and the input voltage step value. However, computing the value of the settling time in a given configuration is not straightforward. The macromodel can give a good estimation, but prototyping can be needed for fine circuit optimization.

5.9 Shutdown function (TSV7723)

The operational amplifier is enabled when the EN pin is pulled high. To disable the amplifier, the EN must be pulled down to VCC-. When in shutdown mode, the amplifier output is in a high impedance state. The EN pin must never be left floating, but must be tied to VCC+ or VCC-.

The turn-on time is calculated for an output variation of ± 200 mV (see Figure 47 & Figure 48. Figure 51 shows the test configurations).

Figure 50. Test configuration



5.10 PCB layout recommendations

Particular attention must be paid to the layout of the PCB tracks connected to the amplifier, load, and power supply. The power and ground traces are critical as they must provide adequate energy and grounding for all circuits. The best practice is to use short and wide PCB traces to minimize voltage drops and parasitic inductance. In addition, to minimizing parasitic impedance over the entire surface, a multi-via technique that connects the bottom and top layer ground planes together in many locations is often used. The copper traces that connect the output pins to the load and supply pins should be as wide as possible to minimize trace resistance.

5.11 Decoupling capacitor

In order to ensure op amp full functionality, it is mandatory to place a decoupling capacitor of at least 22 nF as close as possible to the op amp supply pins. A good decoupling helps to reduce electromagnetic interference impact.

5.12 Macro model

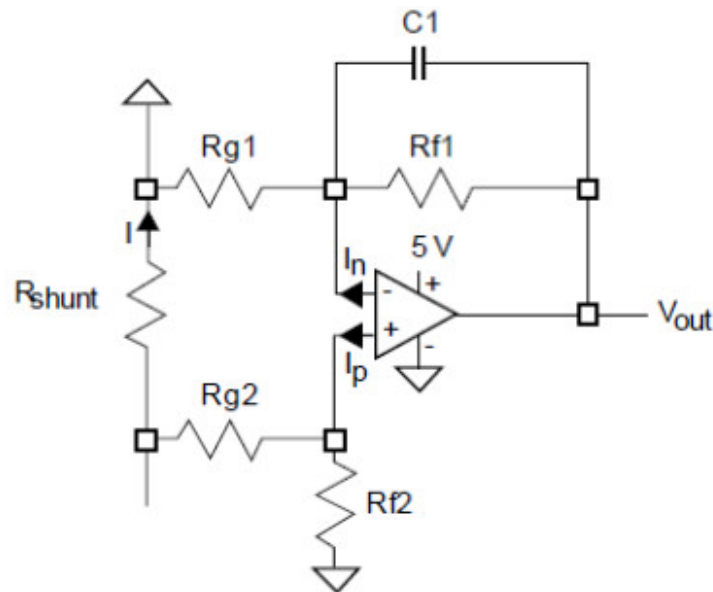
Accurate macro models of the TSV7722 device are available on the STMicroelectronics' website at: www.st.com. These models are a trade-off between accuracy and complexity (that is, time simulation) of the TSV7722 operational amplifier. They emulate the nominal performance of a typical device at 25°C within the specified operating conditions mentioned in the datasheet. They also help to validate a design approach and to select the right operational amplifier, but they do not replace on-board measurements.

6 Typical applications

6.1 Low-side current sensing

Power management mechanisms are found in most electronic systems. Current sensing is useful for protecting applications. The low-side current sensing method consists of placing a sense resistor between the load and the circuit ground. The resulting voltage drop is amplified using the TSV772x (see Figure 51. Low-side current sensing schematic).

Figure 51. Low-side current sensing schematic



V_{out} can be expressed as follows:

$$V_{Out} = R_{shunt} \cdot I \left(1 - \frac{R_{g2}}{R_{g2} + R_{f2}} \right) \cdot \left(1 + \frac{R_{f1}}{R_{g1}} \right) + I_{po} \cdot \frac{R_{g2} \cdot R_{f2}}{R_{g2} + R_{f2}} \cdot \left(1 + \frac{R_{f1}}{R_{g1}} \right) - I_{in} \cdot R_{f1} - V_{io} \cdot \left(1 + \frac{R_{f1}}{R_{g1}} \right)$$

Assuming that $R_{f2} = R_{f1} = R_f$ and $R_{g2} = R_{g1} = R_g$, this equation can be simplified as follows:

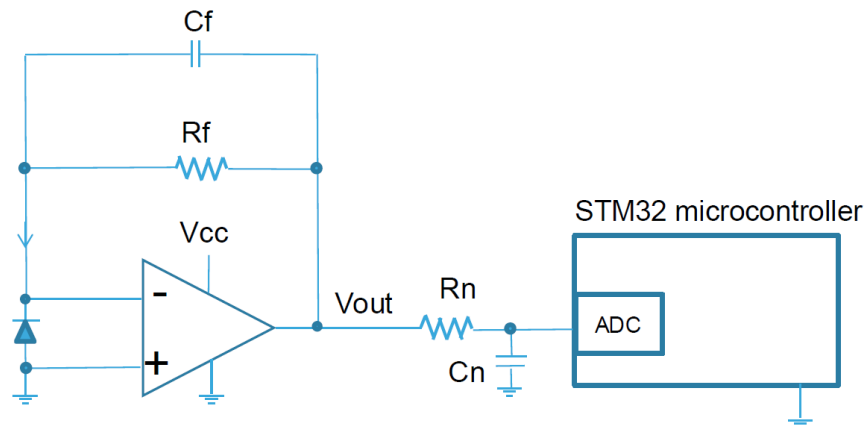
$$V_{Out} = R_{shunt} \cdot I \cdot \frac{R_f}{R_g} - V_{io} \cdot \left(1 + \frac{R_f}{R_g} \right) + R_f \cdot I_{io}$$

The main advantage of using the TSV7722 for a low-side current sensing relies on its low V_{io} , compared to general purpose operational amplifiers. For the same current and targeted accuracy, the shunt resistor can be chosen with a lower value, resulting in lower power dissipation, lower drop in the ground path, and lower cost. Particular attention must be paid to the matching and precision of R_{g1} , R_{g2} , R_{f1} , and R_{f2} , to maximize the accuracy of the measurement. Furthermore, on the TSV7722, the V_{io} is trimmed, and thus reaches his minimum value, at $V_{icm} = 0$ V. This allows optimized precision for low-side current sensing application without precision degradation due to the CMRR.

6.2 Photodiode transimpedance amplification

The TSV7722, with high bandwidth and slew rate, is well suited for photodiode signal conditioning in a transimpedance amplifier circuit. This application is useful in high performance UV sensors, smoke detectors or particle sensors.

Figure 52. Photodiode transimpedance amplifier circuit



The transimpedance amplifier circuit converts the small photodiode output current in the nA range, into a voltage signal readable by an ADC following Eq. (6):

$$V_{Out} = R_f \cdot I_{photodiode}$$

The feedback resistance is usually in the MΩ range, in order to get a large enough voltage output range. However, together with the diode parasitic capacitance, the op amp input capacitances and the PCB stray capacitance, this feedback network creates a pole that makes the circuit oscillate. Using a small (few pF) capacitor in parallel with the feedback resistor is mandatory to stabilize the circuit. The value of this capacitor can be tuned to optimize the application settling time with a SPICE simulation using the op amp macromodel, or by prototyping.

For more details on tuning this circuit, please read the application note AN4451.

7 Package information

In order to meet environmental requirements, ST offers these devices in different grades of **ECOPACK** packages, depending on their level of environmental compliance. ECOPACK specifications, grade definitions and product status are available at: www.st.com. ECOPACK is an ST trademark.

7.1 SOT23-5 package information

Figure 53. SOT23-5 package outline

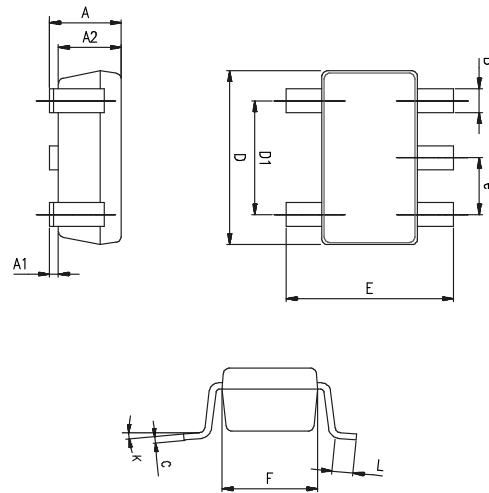


Table 9. SOT23-5 package mechanical data

| Ref. | Dimensions | | | | | |
|------|-------------|------|------|--------|-------|-------|
| | Millimeters | | | Inches | | |
| | Min. | Typ. | Max. | Min. | Typ. | Max. |
| A | 0.90 | 1.20 | 1.45 | 0.035 | 0.047 | 0.057 |
| A1 | | | 0.15 | | | 0.006 |
| A2 | 0.90 | 1.05 | 1.30 | 0.035 | 0.041 | 0.051 |
| B | 0.35 | 0.40 | 0.50 | 0.014 | 0.016 | 0.020 |
| C | 0.09 | 0.15 | 0.20 | 0.004 | 0.006 | 0.020 |
| D | 2.80 | 2.90 | 3.00 | 0.110 | 0.114 | 0.118 |
| D1 | | 1.90 | | | 0.075 | |
| e | | 0.95 | | | 0.037 | |
| E | 2.60 | 2.80 | 3.00 | 0.102 | 0.110 | 0.118 |
| F | 1.50 | 1.60 | 1.75 | 0.059 | 0.063 | 0.069 |
| L | 0.10 | 0.35 | 0.60 | 0.004 | 0.014 | 0.024 |
| K | 0° | | 10° | 0° | | 10° |

7.2 DFN8 2x2 package information

Figure 54. DFN8 2x2 package outline

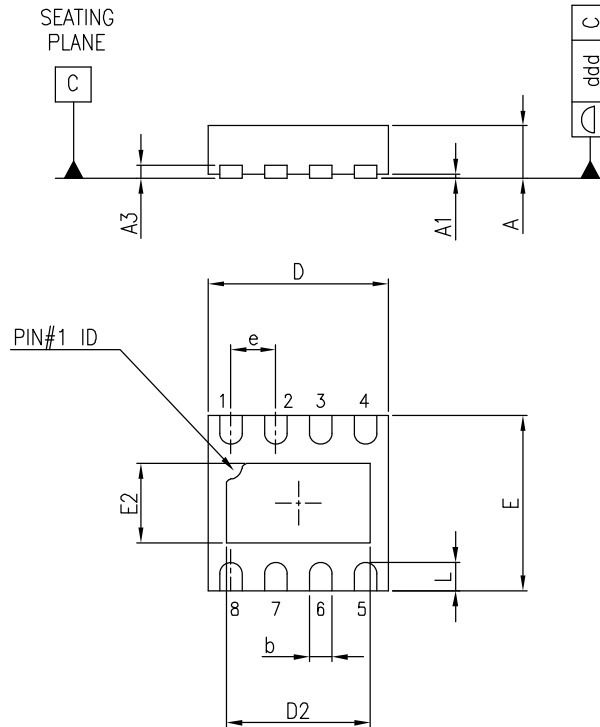
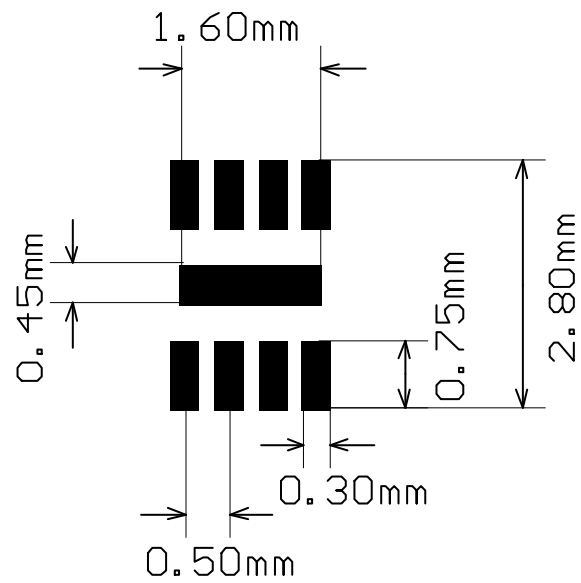


Table 10. DFN8 2x2 package mechanical data

| Ref. | Dimensions | | | | | |
|------|-------------|-------|-------|--------|-------|-------|
| | Millimeters | | | Inches | | |
| | Min. | Typ. | Max. | Min. | Typ. | Max. |
| A | 0.51 | 0.55 | 0.60 | 0.020 | 0.022 | 0.024 |
| A1 | | | 0.05 | | | 0.002 |
| A3 | | 0.15 | | | 0.006 | |
| b | 0.18 | 0.25 | 0.30 | 0.007 | 0.010 | 0.012 |
| D | 1.85 | 2.00 | 2.15 | 0.073 | 0.079 | 0.085 |
| D2 | 1.45 | 1.60 | 1.70 | 0.057 | 0.063 | 0.067 |
| E | 1.85 | 2.00 | 2.15 | 0.073 | 0.079 | 0.085 |
| E2 | 0.75 | 0.90 | 1.00 | 0.030 | 0.035 | 0.039 |
| e | | 0.50 | | | 0.020 | |
| L | 0.225 | 0.325 | 0.425 | 0.009 | 0.013 | 0.017 |
| ddd | | | 0.08 | | | 0.003 |

Figure 55. DFN8 2x2 recommended footprint



Note: The exposed pad of the DFN8 2x2 can be connected to VCC- or left floating.

7.3 MiniSO8 package information

Figure 56. MiniSO8 package outline

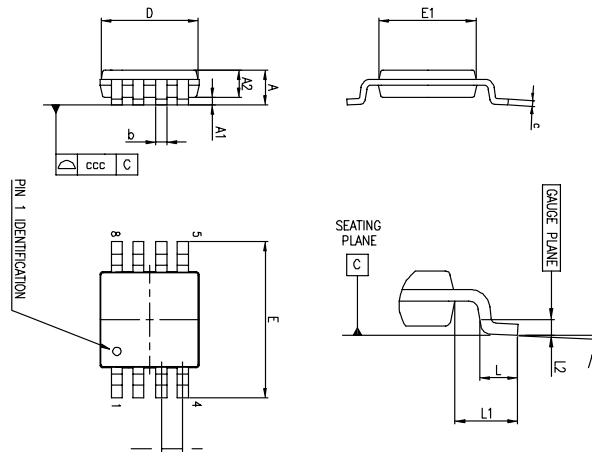
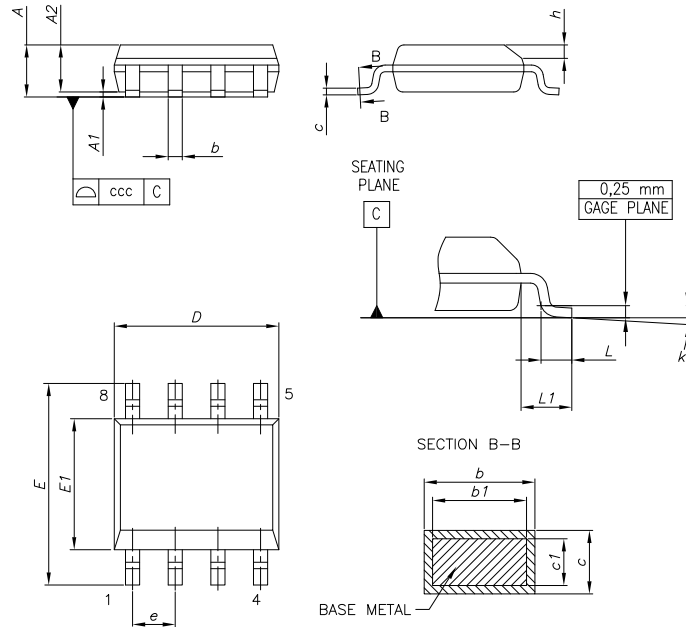


Table 11. MiniSO8 package mechanical data

| Ref. | Dimensions | | | | | |
|------|-------------|------|------|--------|-------|--------|
| | Millimeters | | | Inches | | |
| | Min. | Typ. | Max. | Min. | Typ. | Max. |
| A | | | 1.1 | | | 0.043 |
| A1 | 0 | | 0.15 | 0 | | 0.0006 |
| A2 | 0.75 | 0.85 | 0.95 | 0.030 | 0.033 | 0.037 |
| b | 0.22 | | 0.40 | 0.009 | | 0.016 |
| c | 0.08 | | 0.23 | 0.003 | | 0.009 |
| D | 2.80 | 3.00 | 3.20 | 0.11 | 0.118 | 0.126 |
| E | 4.65 | 4.90 | 5.15 | 0.183 | 0.193 | 0.203 |
| E1 | 2.80 | 3.00 | 3.10 | 0.11 | 0.118 | 0.122 |
| e | | 0.65 | | | 0.026 | |
| L | 0.40 | 0.60 | 0.80 | 0.016 | 0.024 | 0.031 |
| L1 | | 0.95 | | | 0.037 | |
| L2 | | 0.25 | | | 0.010 | |
| k | 0° | | 8° | 0° | | 8° |
| ccc | | | 0.10 | | | 0.004 |

7.4 SO-8 package information

Figure 57. SO-8 package outline



0016023_So-807_fig2_Rev10

Table 12. SO-8 mechanical data

| Dim. | mm | | |
|------|------|------|------|
| | Min. | Typ. | Max. |
| A | | | 1.75 |
| A1 | 0.10 | | 0.25 |
| A2 | 1.25 | | |
| b | 0.31 | | 0.51 |
| b1 | 0.28 | | 0.48 |
| c | 0.10 | | 0.25 |
| c1 | 0.10 | | 0.23 |
| D | 4.80 | 4.90 | 5.00 |
| E | 5.80 | 6.00 | 6.20 |
| E1 | 3.80 | 3.90 | 4.00 |
| e | | 1.27 | |
| h | 0.25 | | 0.50 |
| L | 0.40 | | 1.27 |
| L1 | | 1.04 | |
| L2 | | 0.25 | |
| k | 0° | | 8° |
| ccc | | | 0.10 |

7.5 MiniSO10 package information

Figure 58. MiniSO10 package outline

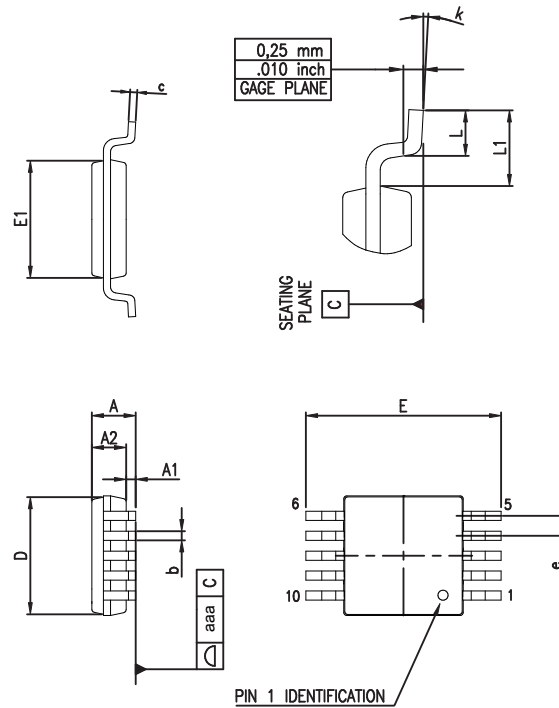


Table 13. MiniSO10 mechanical data

| Ref. | Dimensions | | | | | |
|------|-------------|------|------|--------|-------|-------|
| | Millimeters | | | Inches | | |
| | Min. | Typ. | Max. | Min. | Typ. | Max. |
| A | | | 1.10 | | | 0.043 |
| A1 | 0.05 | 0.10 | 0.15 | 0.002 | 0.004 | 0.006 |
| A2 | 0.78 | 0.86 | 0.94 | 0.031 | 0.034 | 0.037 |
| b | 0.25 | 0.33 | 0.40 | 0.010 | 0.013 | 0.016 |
| c | 0.15 | 0.23 | 0.30 | 0.006 | 0.009 | 0.012 |
| D | 2.90 | 3.00 | 3.10 | 0.114 | 0.118 | 0.122 |
| E | 4.75 | 4.90 | 5.05 | 0.187 | 0.193 | 0.199 |
| E1 | 2.90 | 3.00 | 3.10 | 0.114 | 0.118 | 0.122 |
| e | | 0.50 | | | 0.020 | |
| L | 0.40 | 0.55 | 0.70 | 0.016 | 0.022 | 0.028 |
| L1 | | 0.95 | | | 0.037 | |
| k | 0° | 3° | 6° | 0° | 3° | 6° |
| aaa | | | 0.10 | | | 0.004 |

8 Ordering information

Table 14. Order code

| Order code | Temperature range | Package | Channel | Automotive | Marking |
|-------------|--|----------|---------|------------|----------|
| TSV7721ILT | -40 to +125 °C | SOT23-5 | 1 | | K2A |
| TSV7721IYLT | -40 to +125 °C Automotive grade ⁽¹⁾ | SOT23-5 | 1 | • | K217 |
| TSV7722IQ2T | -40 to +125 °C | DFN8 2x2 | 2 | | K2A |
| TSV7722IST | | MiniSO8 | 2 | | K2A |
| TSV7722IDT | | SO8 | 2 | | TSV7722I |
| TSV7723IST | | MiniSO10 | 2 | | K2A |
| TSV7722IYST | -40 to +125 °C Automotive grade ⁽¹⁾ | MiniSO8 | 2 | • | K217 |
| TSV7722IYDT | | SO8 | 2 | • | TSV7722Y |

1. Qualified and characterized according to AEC Q100 and Q003 or equivalent, advanced screening according to AEC Q001 & Q002 or equivalent. For qualification status detail, check "Maturity Status Link" on first page ("Quality & Reliability" tab on www.st.com).

Revision history

Table 15. Document revision history

| Date | Revision | Changes |
|-------------|----------|--|
| 20-Jan-2021 | 1 | Initial release. |
| 16-Mar-2021 | 2 | <p>Updated the "Related products" table in cover page.</p> <p>Added Section 1 Pin description, Section 1.1 TSV7721 single operational amplifier, Section 1.2 TSV7722 dual operational amplifier and Section 1.3 TSV7723 dual operational amplifier with shutdown option.</p> <p>Changed from 2.5 mA to 2.8 mA for "Maximum supply current $-40\text{ }^{\circ}\text{C} < T < 125\text{ }^{\circ}\text{C}$ and $V_{CC}=5\text{ V}, 3.3\text{ V}, 1.8\text{ V}$".</p> <p>Minor text changes.</p> |
| 25-May-2021 | 3 | <p>Changed name and description pin 5, pin 6 in Figure 3 and Table 3.</p> <p>Updated: V_{IH}, V_{IL}, I_{IH}, I_{IL} parameter in Table 6, Table 7 and Table 8, Figure 20 and Figure 21.</p> <p>Added: Figure 43, Figure 44, Figure 45 and Section 5.9.</p> |
| 13-Oct-2021 | 4 | Updated I_{CC} parameter and max. value row $T = 25\text{ }^{\circ}\text{C}$ in Table 6, Table 8 and Table 10. |
| 15-Nov-2021 | 5 | Updated Figure 41 and Figure 42. |
| 29-Mar-2022 | 6 | Updated title, features and related products on the cover page. |

Contents

| | | |
|----------|--|-----------|
| 1 | Pin description | 2 |
| 1.1 | TSV7721 single operational amplifier | 2 |
| 1.2 | TSV7722 dual operational amplifier | 3 |
| 1.3 | TSV7723 dual operational amplifier with shutdown option | 4 |
| 2 | Absolute maximum ratings and operating conditions | 5 |
| 3 | Electrical characteristics | 6 |
| 4 | Typical performance characteristics | 12 |
| 5 | Application information | 19 |
| 5.1 | Operating voltages | 19 |
| 5.2 | Input offset voltage drift over the temperature | 19 |
| 5.3 | Unused channel | 19 |
| 5.4 | EMI rejection | 19 |
| 5.5 | Maximum power dissipation | 20 |
| 5.6 | Capacitive load and stability | 20 |
| 5.7 | Resistor values for high speed op amp design | 21 |
| 5.8 | Settling time | 22 |
| 5.9 | Shutdown function (TSV7723) | 23 |
| 5.10 | PCB layout recommendations | 23 |
| 5.11 | Decoupling capacitor | 23 |
| 5.12 | Macro model | 23 |
| 6 | Typical applications | 24 |
| 6.1 | Low-side current sensing | 24 |
| 6.2 | Photodiode transimpedance amplification | 25 |
| 7 | Package information | 26 |
| 7.1 | SOT23-5 package information | 27 |
| 7.2 | DFN8 2x2 package information | 28 |
| 7.3 | MiniSO8 package information | 30 |
| 7.4 | SO-8 package information | 31 |
| 7.5 | MiniSO10 package information | 32 |
| 8 | Ordering information | 33 |
| | Revision history | 34 |

List of tables

| | | |
|------------------|---|----|
| Table 1. | Pin description | 2 |
| Table 2. | Pin description | 3 |
| Table 3. | Pin description | 4 |
| Table 4. | Absolute maximum ratings | 5 |
| Table 5. | Operating conditions | 5 |
| Table 6. | Electrical characteristics at $V_{CC+} = 5\text{ V}$, with $V_{CC-} = 0\text{ V}$, $V_{icm} = V_{CC} / 2$, $T = 25^{\circ}\text{C}$, and OUT pin connected to $V_{CC} / 2$ through $R_L = 10\text{ k}\Omega$ (unless otherwise specified) | 6 |
| Table 7. | Electrical characteristics at $V_{CC+} = 3.3\text{ V}$, with $V_{CC-} = 0\text{ V}$, $V_{icm} = V_{CC} / 2$, $T = 25^{\circ}\text{C}$, and OUT pin connected to $V_{CC} / 2$ through $R_L = 10\text{ k}\Omega$ (unless otherwise specified) | 8 |
| Table 8. | Electrical characteristics at $V_{CC+} = 1.8\text{ V}$, with $V_{CC-} = 0\text{ V}$, $V_{icm} = 0.7\text{ V}$, $T = 25^{\circ}\text{C}$, and OUT pin connected to $V_{CC} / 2$ through $R_L = 10\text{ k}\Omega$ (unless otherwise specified) | 10 |
| Table 9. | SOT23-5 package mechanical data | 27 |
| Table 10. | DFN8 2x2 package mechanical data | 28 |
| Table 11. | MiniSO8 package mechanical data | 30 |
| Table 12. | SO-8 mechanical data | 31 |
| Table 13. | MiniSO10 mechanical data | 32 |
| Table 14. | Order code | 33 |
| Table 15. | Document revision history | 34 |

List of figures

| | | |
|-------------------|--|----|
| Figure 1. | Pin connections (top view) | 2 |
| Figure 2. | Pin connections (top view) | 3 |
| Figure 3. | Pin connections (top view) | 4 |
| Figure 4. | Supply current vs. supply voltage | 12 |
| Figure 5. | Input offset voltage distribution at $V_{CC} = 5\text{ V}$ | 12 |
| Figure 6. | Input offset voltage distribution at $V_{CC} = 1.8\text{ V}$ | 12 |
| Figure 7. | Input offset voltage vs. temperature at $V_{CC} = 5\text{ V}$ | 12 |
| Figure 8. | Input offset voltage vs. temperature at $V_{CC}=1.8\text{ V}$ | 12 |
| Figure 9. | Input offset voltage thermal coeff. at $V_{CC}=5\text{ V}$ | 12 |
| Figure 10. | Input offset voltage thermal coefficient at $V_{CC}=1.8\text{ V}$ | 13 |
| Figure 11. | Input offset voltage vs. supply voltage | 13 |
| Figure 12. | Input offset voltage vs. common-mode voltage at $V_{CC} = 5\text{ V}$ | 13 |
| Figure 13. | Input offset voltage vs. common-mode voltage at $V_{CC} = 1.8\text{ V}$ | 13 |
| Figure 14. | Input bias current vs. temp. at $V_{ICM} = V_{CC} / 2$ | 13 |
| Figure 15. | Input bias current vs. common-mode voltage at $V_{CC} = 5\text{ V}$ | 13 |
| Figure 16. | Output current vs. output voltage at $V_{CC} = 5\text{ V}$ | 14 |
| Figure 17. | Output current versus output voltage at $V_{CC}=1.8\text{ V}$ | 14 |
| Figure 18. | Output saturation voltage (V_{OL}) vs. supply voltage | 14 |
| Figure 19. | Output saturation voltage (V_{OH}) vs. supply voltage | 14 |
| Figure 20. | Positive slew rate at $V_{CC} = 5\text{ V}$ | 14 |
| Figure 21. | Negative slew rate at $V_{CC} = 5\text{ V}$ | 14 |
| Figure 22. | Slew rate vs. V_{CC} | 15 |
| Figure 23. | Open loop bode diagram at $V_{CC} = 5\text{ V}$ | 15 |
| Figure 24. | Open loop bode diagram at $V_{CC} = 1.8\text{ V}$ | 15 |
| Figure 25. | Closed loop bode diagram at $V_{CC} = 5\text{ V}$ | 15 |
| Figure 26. | Closed loop bode diagram at $V_{CC} = 1.8\text{ V}$ | 15 |
| Figure 27. | Phase margin vs. common-mode voltage and load current at $V_{CC} = 5\text{ V}$ | 15 |
| Figure 28. | Phase margin vs. capacitive load | 16 |
| Figure 29. | Small step response at $V_{CC} = 5\text{ V}$ | 16 |
| Figure 30. | Small step response at $V_{CC} = 1.8\text{ V}$ | 16 |
| Figure 31. | Desaturation from low rail at $V_{CC} = 5\text{ V}$ | 16 |
| Figure 32. | Desaturation from high rail at $V_{CC} = 5\text{ V}$ | 16 |
| Figure 33. | Settling time output high to low at $V_{CC} = 5\text{ V}$ | 16 |
| Figure 34. | Settling time output low to high at $V_{CC} = 5\text{ V}$ | 17 |
| Figure 35. | Small step overshoot vs. load capacitance | 17 |
| Figure 36. | Linearity vs. load resistance at $V_{CC} = 5\text{ V}$ | 17 |
| Figure 37. | Noise vs. frequency. | 17 |
| Figure 38. | Noise versus time at $V_{CC} = 5\text{ V}$ | 17 |
| Figure 39. | THD+N vs. frequency | 17 |
| Figure 40. | THD+N vs. output voltage | 18 |
| Figure 41. | CMRR vs. frequency at $V_{CC} = 5\text{ V}$ | 18 |
| Figure 42. | PSRR vs. frequency at $V_{CC} = 5\text{ V}$ | 18 |
| Figure 43. | Supply current vs. supply voltage in shutdown mode | 18 |
| Figure 44. | Turn-on time at $V_{CC} = 5\text{ V}$ | 18 |
| Figure 45. | Turn-on time at $V_{CC} = 1.8\text{ V}$ | 18 |
| Figure 46. | EMIRR on In+, In- and Out pins | 20 |
| Figure 47. | Test configuration for R_{ISO} | 21 |
| Figure 48. | Inverting amplifier configuration with parasitic input capacitances | 21 |
| Figure 49. | Settling time measurement configuration | 22 |

| | | |
|-------------------|---|----|
| Figure 50. | Test configuration | 23 |
| Figure 51. | Low-side current sensing schematic | 24 |
| Figure 52. | Photodiode transimpedance amplifier circuit | 25 |
| Figure 53. | SOT23-5 package outline | 27 |
| Figure 54. | DFN8 2x2 package outline | 28 |
| Figure 55. | DFN8 2x2 recommended footprint | 29 |
| Figure 56. | MiniSO8 package outline | 30 |
| Figure 57. | SO-8 package outline | 31 |
| Figure 58. | MiniSO10 package outline | 32 |

IMPORTANT NOTICE – PLEASE READ CAREFULLY

STMicroelectronics NV and its subsidiaries (“ST”) reserve the right to make changes, corrections, enhancements, modifications, and improvements to ST products and/or to this document at any time without notice. Purchasers should obtain the latest relevant information on ST products before placing orders. ST products are sold pursuant to ST’s terms and conditions of sale in place at the time of order acknowledgement.

Purchasers are solely responsible for the choice, selection, and use of ST products and ST assumes no liability for application assistance or the design of Purchasers’ products.

No license, express or implied, to any intellectual property right is granted by ST herein.

Resale of ST products with provisions different from the information set forth herein shall void any warranty granted by ST for such product.

ST and the ST logo are trademarks of ST. For additional information about ST trademarks, please refer to www.st.com/trademarks. All other product or service names are the property of their respective owners.

Information in this document supersedes and replaces information previously supplied in any prior versions of this document.

© 2021 STMicroelectronics – All rights reserved

X-ON Electronics

Largest Supplier of Electrical and Electronic Components

Click to view similar products for [Operational Amplifiers - Op Amps](#) category:

Click to view products by [STMicroelectronics](#) manufacturer:

Other Similar products are found below :

[NCV33072ADR2G](#) [LM358SNG](#) [430227FB](#) [AZV831KTR-G1](#) [UPC824G2-A](#) [LT1678IS8](#) [042225DB](#) [058184EB](#) [UPC259G2-A](#) [UPC258G2-A](#) [NCV33202DMR2G](#) [NTE925](#) [AZV358MTR-G1](#) [AP4310AUMTR-AG1](#) [HA1630D02MMEL-E](#) [HA1630S01LPEL-E](#) [AZV358MMTR-G1](#) [SCY33178DR2G](#) [NJU77806F3-TE1](#) [NCV5652MUTWG](#) [NCV20034DR2G](#) [LM324EDR2G](#) [LM2902EDR2G](#) [NTE778S](#) [NTE871](#) [NTE924](#) [NTE937](#) [MCP6V17T-E/MNY](#) [MXD8015H](#) [MXD8011HF](#) [MXDLN14TP](#) [MXD8921L](#) [MXD8015L](#) [MXDLN16TP](#) [MCP6V16UT-E/OT](#) [MCP6V17T-E/MS](#) [MCP6V19T-E/ST](#) [QCPL-7847-500E](#) [SCY6358ADR2G](#) [LTC2068IUD#PBF](#) [MD1324](#) [CA3140AN](#) [COS8052SR](#) [COS2177SR](#) [COS2353SR](#) [COS724TR](#) [LM2902M/TR](#) [ASOPD4580S-R](#) [ADA4097-1HUIZ-RL7](#) [NCS20282FCTTAG](#)